

# Projection Patterns of Individual X- and Y-Cell Axons From the Lateral Geniculate Nucleus to Cortical Area 17 in the Cat

A.L. HUMPHREY, M. SUR, D.J. UHLRICH, AND S.M. SHERMAN

Department of Neurobiology and Behavior, State University of New York, Stony Brook, New York 11794

## ABSTRACT

Horseradish peroxidase was injected intracellularly into single, physiologically-identified X- and Y-cell geniculocortical axons projecting to area 17 of the cat. This injection anterogradely labeled the axon terminal fields in cortex and retrogradely labeled the somata of these same axons in laminae A and A1 of the lateral geniculate nucleus (LGN). The laminar projections of 21 X- and 15 Y-cell axons were analyzed. For these, the laminar terminations of ten X- and seven Y-cell axons were also related to their cells' positions in the A-laminae.

The terminal fields of X- and Y-cell axons overlapped substantially in layers IV and VI of area 17. Some X-cells terminated mainly in IVb, others mainly in IVa, and still others throughout IVa and IVb. The latter two groups also projected up to 100  $\mu\text{m}$  into lower layer III. Y-cells terminated primarily in layer IVa and projected up to 200  $\mu\text{m}$  into lower layer III. Some also arborized throughout the depth of layer IVb. Both X- and Y-cell axons terminated throughout the depth of layer VI, although more so in the upper half. We found no relationship between the diameter of the parent axon and its sublaminar projection within layer IV.

Within layer IV, X-cell axons generally terminated within a single, continuous clump and had surface areas of 0.6 to 0.9  $\text{mm}^2$ . Axons of Y-cells often terminated in two to three separate clumps, separated by terminal free gaps 400 to 600  $\mu\text{m}$  wide. Their total surface areas, including gaps, were 1.0 to 1.8  $\text{mm}^2$ , roughly 1.6 times the surface areas of X-cell axons. Despite considerable overlap, Y-cell arbors contained significantly more boutons than did X-cell arbors.

The sublaminar projections of the X- and Y-cell axons within layer IV reflected the locations of the cells' somata within the depth of the A-laminae. X-cells located in the dorsal or ventral thirds of the depths of the laminae projected mainly to layer IVa or throughout layer IV in cortex. Those located in the central thirds projected mainly to layer IVb. Y-cells showed a similar positional relationship, but they appeared to follow different rules. Y-cells in the outer thirds of the A-laminae projected mainly to layer IVa; those in the central thirds, in addition, expanded their projections to include layer IVb.

In general, larger sized somata in the LGN gave rise to more widely spreading terminal arbors and greater numbers of boutons in cortex than did smaller somata. However, we found no significant relationship between soma size and terminal arbor extent or total boutons within each cell class (X or Y), and thus the correlation noted may result from Y-cells having larger somata and terminal arbor extents than do X-cells.

Our results demonstrate considerable heterogeneity in the laminar projections of X- and Y-cell axons within area 17. This heterogeneity reflects an underlying sublaminar organization of the parent somata within the depths of the LGN A-laminae. The functional significance of this organization, both

Accepted September 27, 1984.

M. Sur's present address is Section of Anatomy, Yale University School of Medicine, New Haven, CT 06510.

in the LGN and cortex, is unknown. It is clear, however, that the result of the geniculocortical projection upon layer IV is not to segregate X- and Y-afferents into lower and upper tiers. Rather, it may be to re-establish a positional organization existing within the depths of the LGN laminae.

**Key words:** laminar terminations, soma locations, arbor extents, numbers of boutons, axon diameters

Three major classes of neurons in the cat, called X-, Y-, and W-cells, form separate, parallel pathways of visual information flow from the eye to cortex (see reviews by Stone et al., '79; Lennie, '80; Sherman and Spear, '82; Sherman, '84). The different pathways arise from morphologically distinct retinal ganglion cells (Boycott and Wässle, '74; Cleland et al., '75; Peichl and Wässle, '81; Wässle et al., '81a,b; Saito, '83; Stanford and Sherman, '84) that in turn project to different populations of cells in the dorsal lateral geniculate nucleus (LGN) (Cleland et al., '71; Hoffmann et al., '72). There is little or no direct convergence among the different classes of retinal afferents onto single geniculate cells (Cleland et al., '71; Hoffmann et al., '72).

The X-, Y-, and W-cells are uniquely distributed within the lateral geniculate nucleus (see reviews by Stone et al., '79; Lennie, '80; Sherman and Spear, '82; Sherman, '84). X-cells are restricted primarily or exclusively to the A-laminae, although some may exist in lamina C and the medial interlaminar nucleus (MIN; the MIN is a subdivision of the LGN). Y-cells are present throughout the A-laminae, lamina C, and the MIN. W-cells are found in the C-laminae, although some may also exist in the MIN and the geniculate wing adjacent to the MIN. The projections of neurons from the LGN to the different visual cortical areas are also unique, because a cell's projection pattern is dependent upon both its physiological type and its location within the different subdivisions of the LGN.

Extracellular tracer studies (Rosenquist et al., '74; LeVay and Gilbert, '76; Leventhal, '79) have revealed that geniculate neurons in laminae A and A1 project to layers IV and VI of cat area 17. These results raised the possibility that the X- and Y-cell classes might have different sublaminar projection patterns in visual cortex. This possibility was tested by Ferster and LeVay ('78) with anatomical methods. Geniculate neurons were retrogradely filled from bulk injections of horseradish peroxidase (HRP) above the LGN. Geniculate cells with class 1 morphology, believed to be Y-cells, were found to have large axons (2.0  $\mu\text{m}$ ), while class 2 cells, believed to be X-cells, had medium axon diameters (1.0 to 1.5  $\mu\text{m}$ ). Bulk extracellular injections of HRP were then made in the white matter below area 17 to anterogradely fill the terminal fields of axons projecting into cortex. One population of axons projecting mainly to upper layer IV and deep layer III had large axons and were presumed to be Y-cell axons, while another population, which projected to lower layer IV, had medium axons and were presumed to be X-cell axons. Ferster and LeVay ('78) concluded that geniculate X- and Y-cell axon projections are segregated into the lower and upper halves of layer IV, respectively, with little or no overlap. These conclusions were basically supported by Bullier and Henry ('79c), who used similar anatomical methods, although they showed that some X-cell arbors also rose into the lower half of layer IVa. A possible X-cell input to lower layer III (as well as

lower layer IV) was reported by Leventhal ('79) using anatomical methods. Gilbert and Wiesel ('79, '83), by use of intracellular injections of HRP into functionally identified X- and Y-cell axons, reported confirmation of the original observations of Ferster and LeVay ('78).

Recent anatomical and physiological studies have led us to question some of the established beliefs about these laminar projection patterns. Friedlander et al. ('81) injected HRP intracellularly into physiologically identified geniculate neurons and confirmed that X- and Y-cells differ morphologically. However, these authors found that while many Y-cells in the LGN possess the class 1 morphology, some exhibit class 2 features. Also, the axon diameters of X- and Y-cells overlap to some extent, making it difficult to use axon diameter in cortex as the sole criterion for determining the X- or Y-cell derivation of the axon. It has also been shown that layer IV in the cat receives a strong projection from the visual claustrum (LeVay and Sherk, '81). One would thus expect axons from the claustrum as well as from the LGN to be labeled by HRP injections into the white matter under cortex.

The above questions and issues led us to re-examine the termination patterns of geniculate neurons in areas 17 and 18 by injecting HRP into single, physiologically identified X- and Y-cell axons. The parent cells of the injected axons were also retrogradely labeled. This allowed us to relate a cell's soma size and position in the LGN to both the cortical area to which it projected, as well as to the size, shape, and laminar distribution of its axon terminal field. In this paper we shall describe the area 17 projection patterns of X- and Y-cells from laminae A and A1 of the LGN. Our main conclusions are that X- and Y-cell axons arborize throughout layers IV and VI, intermingling substantially with one another, and that these cells' sublaminar projections upon layer IV are related to the locations of their somata within the depths of the A-laminae. In the accompanying paper (Humphrey et al., '85), we describe the patterns of geniculate axonal projections to area 18, those to the 17-18 border region, and those that branch to innervate areas 17 and 18. Preliminary results of this work have appeared in abstract form (Humphrey et al., '82, '83; Humphrey and Uhlrich, '84).

## METHODS

The general methods for surgical preparation, visual stimulation, recording, cell classification, and HRP iontophoresis are similar to those described previously from our laboratory (Friedlander et al., '81; Sur and Sherman, '82; Stanford et al., '83).

### General preparation

Adult cats (2.0 to 4.0 kg) were anesthetized with 4% halothane in a 50/50 mixture of nitrous oxide and oxygen. We cannulated the femoral vein for infusion of paralytics,

performed tracheotomy to insert an endotracheal tube, and administered 1.0 mg atropine sulfate (i.m.) to minimize mucous secretion. The animal was then placed in a stereotaxic apparatus, paralyzed with 5 mg of gallamine triethiodide, and maintained on a continuous infusion of paralytics (3.6 mg/hour g. triethiodide, 0.7 mg/hour d-tubocurarine and 6 ml/hour of 5% lactated Ringer solution). The cat was artificially ventilated, expired carbon dioxide was continuously monitored and kept at about 4%, and the animal's rectal temperature was maintained at 37.5 to 38.0°C using a feedback controlled heating pad. During the stereotaxic surgery the animal was maintained on 1.0 to 1.5% halothane and a 60/40 mixture of nitrous oxide and oxygen. All wound margins, pressure points, and underlying musculature were infused with 1% lidocaine and heart rate was monitored throughout the experiment. Upon completion of the craniotomies and placement of the stimulating electrodes, halothane was discontinued, and the animals were maintained on a 70/30 mixture of nitrous oxide and oxygen. For animals in the latter half of this series of experiments, Nembutal was also added to the infusion solution at a rate of 1 mg/kg·hour. All geniculocortical axons responded briskly and consistently under these anesthetic levels.

### Electrical stimulation

In most experiments, bipolar stimulating electrodes (tungsten wire coated with Insl-X except for 0.5 to 1.0 mm exposed at the tips) were placed in the optic chiasm and in the optic radiation just above the LGN in order to determine the range of conduction latencies of the X- and Y-cell axons. In early experiments, only the chiasm electrodes were used; these were inserted at anterior 14.0 mm and lateral 1.5 mm on each side to straddle the chiasm. To ensure valid and reliable latency measures within and across animals the electrodes were not cemented in place until the photically evoked field potential at the chiasm was pronounced (roughly 10 mV) and clearly evoked by stimulation of either eye.

Similar care was taken to place the optic radiation electrodes in the anterior portion of the LGN, where the lower visual fields are represented. We used a micropipette filled with 3 M KCl to locate the top of lamina A and to determine the location of the geniculate receptive fields there. This information was then used in conjunction with Sanderson's ('71) maps of the LGN to position the stimulating electrodes such that the medial electrode was over the geniculate region roughly representing the vertical meridian and  $-5^\circ$  elevation, and the lateral electrode was over the representation of roughly  $30^\circ$  azimuth and  $-8^\circ$  elevation. The stimulating electrodes were then lowered, using the field potentials evoked by optic chiasm stimulation, to place the tips of the electrodes 0.5 to 1.0 mm above the surface of lamina A. All radiation electrode placements were verified histologically.

Current pulses (0.01 to 0.1 msec; 1 to 5 mA at radiations and 2 to 10 mA at chiasm) were passed between each electrode in the pair to elicit orthodromic activation of the geniculocortical axons. Latency, measured on a storage oscilloscope, was taken as the time from onset of the stimulus artifact to the foot of the action potential (Bishop et al., '62a). No latency jitter was associated with repeated activation from the radiation electrodes since no synapses were involved. A small amount of jitter (0.1 to 0.3 msec for X-cell axons and 0.1 to 0.2 msec for Y-cell axons) was observed

with chiasm stimulation. The shortest repeatable latencies observed from chiasm stimulation were used, in accordance with previous studies (Bullier and Henry, '79a-c).

### Visual stimulation

The pupils were dilated by topical application of 1% atropine sulfate (ophthalmic), and the corneas were covered with contact lenses whose curvature, as judged by retinoscopy, focused the animals' retinas onto a frontal tangent screen or cathode ray tube used for visual stimulation. We plotted the receptive fields of the X- and Y-cell axons on the tangent screen. Receptive field position relative to the optic discs and hence to the vertical and horizontal meridians was determined using standard methods (Bishop et al., '62b; Fernald and Chase, '71). The accuracy is within  $2.0^\circ$ . Responses to spatial sine wave gratings sinusoidally modulated in time were used to determine the spatial and temporal summation properties of the cells. The gratings were generated on a cathode ray tube with a mean luminance of 38 cd/m<sup>2</sup> and a grating contrast of 0.6; spatial frequency, temporal frequency, and spatial phase were continuously variable. Cells were considered to sum linearly if their responses occurred predominantly at the fundamental temporal frequency of the stimulus and showed a sinusoidal spatial phase dependency; the latter property usually included a grating position at which no responses above background were evident (i.e., the "null position"). Cells with nonlinear summation exhibited a frequency-doubled response that was largely independent of spatial phase. Many cells did not exhibit clearly nonlinear responses at lower spatial frequencies, but if they did so at higher ones, they were considered to be nonlinear (Hochstein and Shapley, '76; So and Shapley, '79).

### Electrophysiological recording and cell classification

Axons were recorded using glass micropipettes filled with a solution of 4 to 6% HRP (Sigma Type VI) in 0.2 M KCl and 0.05 M Tris, buffered to pH 7.4. The pipette tip was bevelled to produce a final impedance of 75 to 105 Mohm at 100 Hz. The electrodes were inserted into the brain along the lateral gyrus through small (2 to 3 mm diameter), hydraulically sealed craniotomies. The mediolateral placement was chosen so the electrode would travel for 2 to 4 mm through the white matter beneath areas 17 and 18 and thereby maximize the chances of recording from the parent trunk of a geniculocortical axon rather than from one of its collateral branches in the gray matter. Injections along the parent trunk generally result in more complete labeling of the whole terminal field than injections of the more distal branches.

On the basis of extracellular recording, we could readily distinguish geniculocortical axons from other presumably cortical or extrageniculate axons in the optic radiations and gray matter. Compared to these other axons, geniculate cells generally have higher spontaneous activity, are more briskly driven, and have monocular, orientation nonselective receptive fields with center/surround organization. Also, geniculate cells generally are more readily activated electrically from the optic chiasm and radiation electrodes with shorter latencies than are nongeniculate axons. While recording extracellularly, a range of properties was used to identify the axon as X or Y (see Sherman and Spear, '82). The main criterion used was the response to counterphased

sine wave gratings. Generally, X-cells show linear summation in response to counterphased sine wave gratings, whereas Y-cells sum nonlinearly. Additional, confirmatory properties included the following. At a given visual field eccentricity, X-cell receptive field centers are smaller than those of Y-cells; X-cells respond in a more sustained fashion than do Y-cells to standing contrast; X-cells have stronger antagonistic surrounds than do Y-cells; and X-cells do not respond as well as do Y-cells to targets moved rapidly ( $>200^\circ/\text{second}$ ) through the field. In any cases where cell classification based on these latter response properties differed from that based on the linearity test, the cell was classified on the basis of the linear or nonlinear summation. We also noted the location of the receptive field in space and the eye through which the cell was driven. Finally, we determined the latency of the axon's response to electrical stimulation of the optic chiasm. When optic radiation electrodes were used, we also determined response latency to radiation stimulation, and the latency difference between chiasm and radiation stimulation was computed and used to distinguish X- and Y-cell axons.

Once characterized extracellularly, the axon was impaled by slowly advancing the electrode and passing short bursts of positive current (2 to 3 nA). Penetration was indicated by a rapid 30 to 50 mV drop in the potential and large ( $>10$  to 20 mV) positive, monophasic action potentials. HRP was then iontophoresed by injecting positive current pulses (3 to 10 nA) of variable frequency and duty cycle across a bridge circuit. The duration of successful injections varied from 30 seconds to 10 minutes. The bridge circuitry enabled us to monitor each cell's activity during iontophoresis; throughout the injection the axon's receptive field properties were repeatedly checked to ensure it was the same as that noted extracellularly. The injection was terminated either when the resting potential decayed by roughly half or when it was felt that sufficient HRP had been iontophoresed. At this point a burst of negative current (3 to 5 nA) was applied and the electrode was rapidly withdrawn, producing a sharp rise in potential. Following a successful injection, the electrode was removed and a new penetration started at least 2 mm distant along the anteroposterior axis of the lateral gyrus.

Following the last injection, the animal was maintained for at least an additional 14 hours, thereby allowing retrograde transport of the HRP to the parent somata in the LGN. The postinjection survival times for different axons ranged between 14 and 40 hours. Within this time, we saw no deterioration in the quality of anterograde labeling in the axon terminal fields nor any indication of leakage of HRP from axon terminals in cortex or labeled somata in the LGN.

### Histology

After sufficient survival time the animals were given 100 mg of sodium pentobarbital i.v. and perfused through the ascending aorta with 2 liters of 1% paraformaldehyde and 2% glutaraldehyde in 0.1 M phosphate buffer (pH 7.4) followed by 500 ml of 10% sucrose in buffer. The brain was then blocked stereotaxically and placed in 30% sucrose overnight. Serial coronal sections (100  $\mu\text{m}$  thick) were cut on a freezing microtome. The cortical sections were reacted in diaminobenzidine (DAB) with cobalt chloride intensification (Adams, '77), and the LGN sections were reacted in O-dianisidine (de Olmos, '77).

### Reconstructions

Four criteria were employed to select an axon for reconstruction: the injection had been made in the white matter or in lower layer VI; the injection site was clear of major debris; a single axon emerged from either side of the injection site; and the axon was well enough labeled that its boutons were readily visible under the microscope at  $250\times$ . A number of axons failed this last criterion, due largely to their being injected for an insufficient time. Most axons were reconstructed from drawings of serial coronal sections using a drawing tube attachment on a microscope at a magnification of 400 or 500. A few were so well labeled and their boutons were so distinct that they were reconstructed at a magnification of 250.

Measurements of axon diameters were made at a magnification of 1,000 (with an oil immersion objective of  $100\times$ , N.A. 1.32). We measured the parent axon rather than the smaller primary axon collaterals. In some cases in which only the primary collaterals were labeled well, no measurements of axon diameter were taken. For each axon, four to ten measurements were taken roughly 100  $\mu\text{m}$  apart (generally near the cut edges of the sections); these measurements were averaged and rounded to the nearest 0.5  $\mu\text{m}$  (Friedlander et al., '81).

The retrogradely filled cells in the LGN were labeled well enough to draw the outline of their somata and to determine cell surface area. It was not possible to continuously follow an injected axon in cortex to its soma in the LGN. Instead, Sanderson's ('71) maps of the LGN were used to match each geniculate cell to its axon in cortex on the basis of soma location, receptive field position, and ocular dominance. To ensure unambiguous soma-axon matches, only three to five geniculocortical axons were injected in each hemisphere, only two to three related to each eye, and receptive field locations were at least five to  $10^\circ$  apart unless they differed in ocular dominance. Every geniculate cell could be matched to an axon in cortex. For three injections (out of 109), two adjacent LGN cells were found; in each case these were due to having inadvertently filled two adjacent axons in cortex. These soma axon pairs were excluded from our analysis.

After reconstructing an axon, the sections were counterstained for Nissl substance with cresyl violet or, in a few cases, with neutral red. Laminal and areal boundaries were determined according to the cytoarchitectonic criteria of O'Leary ('41), Otsuka and Hassler ('62), and Lund et al. ('79). Identifying the boundary between areas 17 and 18 was also aided by noting the receptive field positions of cells encountered in the gray matter at the beginning of electrode penetrations.

Since our results concerning the laminar projections within layer IV of X- and Y-cell axons differ from those of previous studies, we will briefly review the criteria for determining the borders of the layer. Figure 1 illustrates the cytoarchitecture of area 17 and our placement of laminar boundaries. Layer IV consists of two subdivisions of roughly equal thickness, designated IVb and IVa, after O'Leary ('41) and Lund et al. ('79). These are equivalent to layers IVab and IVc, respectively, of Otsuka and Hassler ('62). Layer IVb consists of tightly packed, small stellate cells and a few small pyramidal-shaped cells. Its ventral border occurs at the level of the apices of the most superficial pyramids in layer Vb which invade layer Va, a narrow sublamina of small and medium pyramidal-shaped cells

immediately below IVb. Layer IVa consists of more loosely packed, small and medium sized stellate and pyramidal cells. At its dorsal border with layer III, large pyramidal cells are present whose initial apical dendrites are readily visible in Nissl stained sections. We placed the layer III-IV border at the base of these pyramids. The boundary between sublayers IVa and IVb is apparent by the differences in cell size and density in the two subdivisions and by the occasional appearance of large, round, or oval-shaped cells, which are present at the base of layer IVa.

Most geniculate axons arborized over 10 to 20 consecutive sections and frequently the laminar boundaries determined for one portion of the field did not accurately reflect the boundaries in another portion. This was due mainly to the sections not being cut exactly perpendicular to the laminar planes. Therefore, it was necessary to determine the laminar boundaries for each section through the terminal field in order to localize the boutons accurately in the different sublaminae. This was done for each axon, irrespective of

the plane of section. In some of the two dimensional reconstructions of the complete terminal fields presented below, a few processes have been slightly shifted vertically to reflect more accurately their true laminar position. In reconstructions where the laminar distortions were larger, the boundaries are illustrated on single sections. All reconstructions and measurements are uncorrected for linear shrinkage of the tissue, which we estimate to be about 15%.

### Statistics

Unless otherwise indicated, statistical comparisons were done using the Mann-Whitney U-test (Krauth, '83).

### RESULTS

We recorded extracellularly from 228 geniculocortical axons, identified them as arising from 113 X- and 115 Y-cells, characterized their receptive field properties, and determined their latencies of response to electrical stimulation. Of these, 106 were labeled by intracellular iontophoresis of

## Area 17

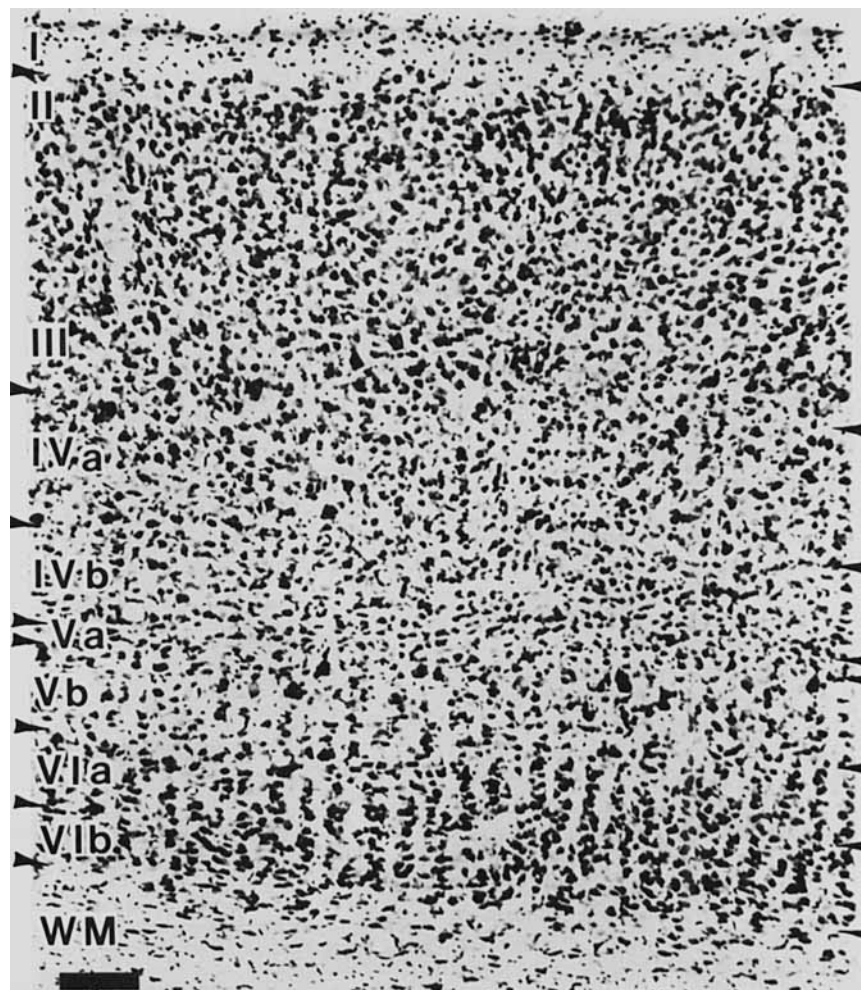


Fig. 1. Photomicrograph of coronal section of cat area 17 stained for Nissl substance. The laminar boundaries are numbered according to O'Leary ('41). See text for further description. Scale bar = 100  $\mu$ m.

HRP, and all but nine of these were labeled sufficiently to backfill their somata in the LGN. We found it much easier to label the somata of injected axons retrogradely than to label their terminal fields completely. Nevertheless, 35 X- and 54 Y-cell axons were sufficiently well labeled antero-gradely to determine whether they projected to area 17 and/or to area 18. For the area 17 projecting axons, the terminal arbors of 21 X- and 15 Y-cells were labeled adequately enough to examine their laminar projections. For this group, 12 X- and seven Y-cell arbors were labeled particularly well, and we focused on these for a more quantitative analysis of laminar projections. Most of our conclusions are based on this latter group and are supported by the other, less completely labeled, axons.

We shall first describe the distribution of response latencies to electrical stimulation for the X- and Y-cell axons and then illustrate the laminar and areal projection patterns of single X- and Y-cell axons in area 17 and relate these to their soma locations in the LGN.

### Conduction latencies

Bullier and Henry ('79b) noted that the latencies of a cortical cell's responses to stimulation of the optic chiasm and radiations, particularly the latency differences between these two responses, were useful for detecting the X- or Y-cell inputs to the cell. This latency difference, designated as the (OX-OR) latency, reflects the sum of transmission time between the chiasm and the geniculate neuron, retinogeniculate synaptic delay, and conduction time over the short distance from the LGN neuron to the radiation electrodes just above lamina A.

Figure 2A,B shows the total distribution of (OX-OR) latencies for 228 X- and Y-cell axons recorded in the optic radiations beneath areas 17 and 18, or within each area itself. Latency differences for Y-cell axons ranged from 0.5 to 1.8 msec, and for X-cell axons, from 1.3 to 2.5 msec. All but three of the overlapping (OX-OR) latency values for the X- and Y-cell population were restricted to a small range of latencies between 1.4 and 1.6 msec, with greatest overlap at 1.5 msec. All but one of the axons with latency differences less than 1.4 msec were Y-cells and all but two of the axons with latency differences greater than 1.6 msec were X-cells. Thus, outside of the overlap range of 1.4 to 1.6 msec, the (OX-OR) latency alone is a reliable predictor of an axon's physiological class. However, 59 axons (26%) had (OX-OR) latency differences of 1.4 to 1.6 msec.

Figure 2C,D shows the distribution of (OX-OR) latencies for Y-cell axons that projected to area 17 or to area 18. Fewer axons are represented in these histograms than in Figure 2A because Figure 2C,D represents the subpopulation of axons that were either injected and traced anatomically to one of the cortical areas or were recorded within the area itself. Figure 2A, on the other hand, also includes data from axons whose cortical area of termination could not be determined. Despite considerable overlap in (OX-OR) latencies, Y-cell axons that projected to area 17, on the average, had significantly larger latency differences than those innervating area 18 ( $P < .001$ ). Further differences between geniculocortical projections to areas 17 and 18 are considered in the accompanying paper (Humphrey et al., '85).

For the axons that project to area 17, X- and Y-cells exhibit moderate overlap in their (OX-OR) latencies (Fig. 2B,C). For roughly one-third each of the X- and Y-cell axons

latency alone is a poor predictor of functional class. Conversely, roughly two-thirds of the axons can be identified clearly as X or Y by their latency values. Our results thus confirm the conclusions of Bullier and Henry ('79b,c) that, outside a small range, the (OX-OR) latency is a valid and reliable measure for distinguishing these two pathways which innervate cortex.

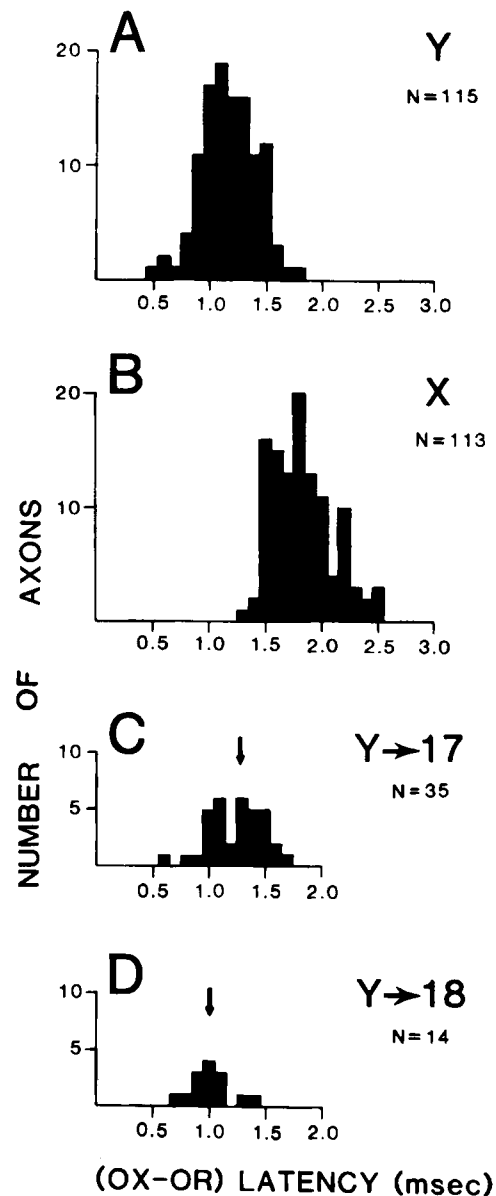


Fig. 2. Histograms summarizing the (OX-OR) latencies for 228 X- and Y-cell axons recorded in cortex. A. Latencies for all of the recorded Y-cell axons, irrespective of cortical area of termination. B. Latencies of all recorded X-cell axons. C. Latencies of Y-cell axons that were either recorded within area 17 or that were injected and subsequently traced to that area. Arrow marks the median latency of 1.3 msec. D. Latencies of Y-cell axons that were recorded in, or traced to, area 18. Arrow marks the median latency of 1.0 msec. The (OX-OR) latencies of Y-cells that project to area 17 are significantly larger on the average than those projecting to area 18.

### Overview of geniculate somata and terminal arbors in area 17

Figure 3 shows photomicrographs of typical HRP-filled X- and Y-cell terminal arbors in layer IV. Arbors of X- and Y-cells were virtually indistinguishable from one another at the light microscopic level. For both, the arbors consist mainly of very fine axon collaterals, less than  $0.5 \mu\text{m}$  in diameter, that are studded with numerous boutons en passant and that end with a single bouton (Fig. 3A,C). Only occasionally do they occur in clusters of five to 15 (Fig. 3B,D). The boutons are  $0.5$  to  $2.0 \mu\text{m}$  in diameter (average =  $1.0 \mu\text{m}$ ). Each bouton has been shown by electron microscopy to form one to three synapses with postsynaptic structures (LeVay, '73; Winfield and Powell, '83; Einstein et al., '83a,b; Tieman, '84). Thus, the number of synapses associated with each of the terminal arbors shown below may be much greater than the number of boutons. The similarity in the light microscopic appearance of geniculocortical X- and Y-cell terminal arbors can be contrasted against the differences in appearance between retinogeniculate X- and Y-cell arbors (Sur and Sherman, '82).

Figure 4 shows photomicrographs of typical X- and Y-cell somata in the LGN that were labeled retrogradely after injecting HRP into their axons in cortex. They often exhibited granular filling with HRP, which is typical of retrograde transport. The outline of the soma was always quite clear, allowing accurate measurements of soma size. In the more densely labeled cells, many primary dendrites, a few secondary dendrites, and the proximal portion of the axon were also visible. However, we have not been able to label the more distal dendrites and thus cannot usually relate the morphology of any of our labeled cells to prior morphological classifications (Guillery, '66; Friedlander et al., '81).

#### X-cell projections to area 17

All of the X-cell axons in our sample arose from cells in lamina A or A1 of the LGN and either projected to area 17 only, or projected to areas 17 and 18 by extending across the 17-18 border region. Only the former will be considered in this paper; the latter are dealt with in the following paper (Humphrey et al., '85). Within area 17, there was considerable heterogeneity in the sublaminar distributions of X-cell axons, with some projecting primarily to layer IVb, others primarily to layer IVa, and still others projecting throughout layer IV. For the latter two groups, the projections also included deep layer III. Thus, X-cell input is not restricted to the lower half of layer IV as previously suggested (e.g., Ferster and LeVay, '78). X-cell axons also terminate throughout layer VI.

**X-cell projections to layer IVb.** An X-cell axon with an arborization mainly in lamina IVb is illustrated in Figure 5. This projection pattern was seen in four out of the 12 X-cell axons that were reconstructed in detail. (For this and the following examples of geniculocortical projections, the physiological properties of the cells are summarized in the figure legends.) The parent axon was recorded and injected just below the terminal arbor (arrow in Fig. 5A). The parent was traced ventrally and anteriorly for about 5 mm into the white matter to a point near the base of the splenial sulcus, where it became too lightly labeled to follow further. However, knowledge of the axon's receptive field location and ocular dominance allowed us to identify unequivocally its soma in lamina A of the LGN (Fig. 5B). The label clearly reveals the cell's soma, the intrageniculate portion of its

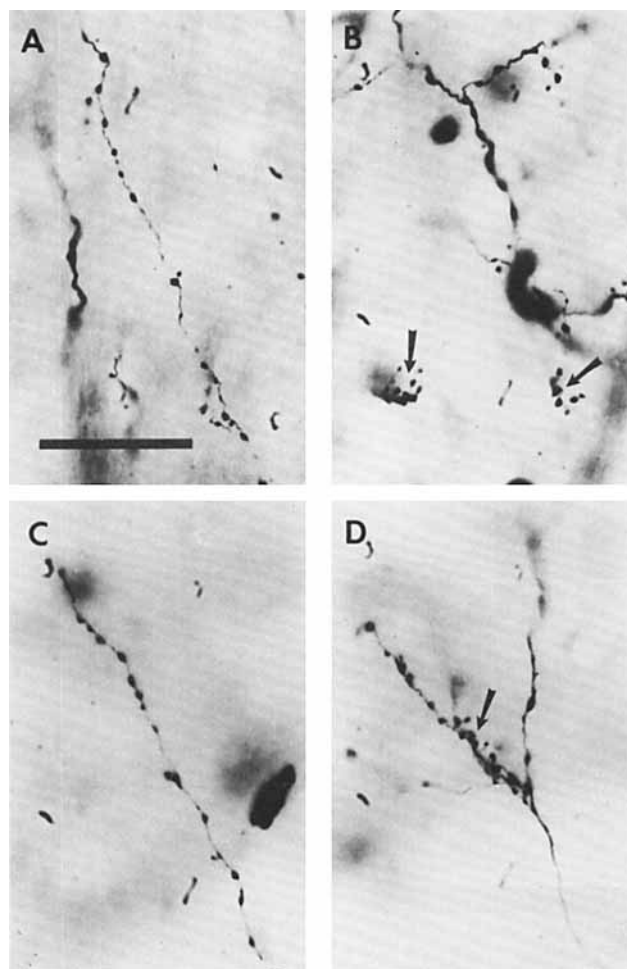


Fig. 3. High power photomicrographs of the terminal processes of an X- and a Y-cell axon in layer IV of area 17. A. Small process of an X-cell axon distributing boutons en passant. Scale bar =  $50 \mu\text{m}$  and applies to B-D. B. Small clusters (arrows) of 5 to 10 boutons within the X-cell arbor. C. Boutons en passant distributed by a Y-cell axon. Note their similarity in size and distribution to the boutons in A. D. Cluster of boutons (arrow) near a branch point in the Y-cell arbor.

axon, and a number of proximal dendrites (Fig. 5C). The cell's soma is large, being  $407 \mu\text{m}^2$  in cross-sectional area, but is within the range of X-cell soma sizes observed by Friedlander et al. ('81).

This X-cell's terminal arbor in cortex is illustrated in greater detail in Figure 5D. As is typical with many X-cells we have observed, the first bifurcation of the parent axon occurred in the white matter close to the termination site. A few bouton-laden processes were given off in layer VIa, but the majority arborized densely in layer IVb. Here many of the processes travelled horizontally up to  $500 \mu\text{m}$ , giving off smaller branches along their course, each of which was studded with boutons. Examples of these boutons are illustrated in Figure 6. In addition to the layer IVb arbor, a number of processes arborized in layer IVa, mainly in the lower half. Figure 6A,B shows photomicrographs of some of these processes relative to the cytoarchitectonic boundaries of layer IVa. One small process rose to the level of the layer

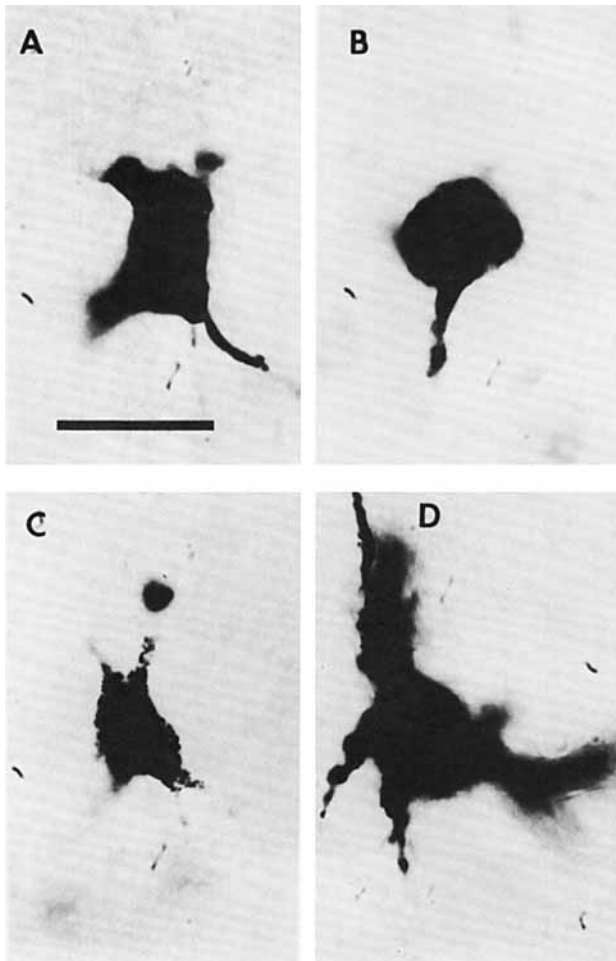


Fig. 4. Photomicrographs of retrogradely labeled X- and Y-cells in the A-laminae whose axons were injected in cortex and traced to area 17. A, B. Two X-cells located in lamina A. The complete outline of the soma and labeled dendrites for the cell in A is shown in Figure 5C. Scale bar in A = 50  $\mu\text{m}$  and applies to B–D. C. Y-cell in lamina A1. D. Y-cell located in the interlaminar zone between lamina C and the medial interlaminar nucleus. The somata are densely labeled, frequently obscuring the HRP-granules (except in C), and their outlines are clearly visible. The primary dendrites are also variably labeled. Soma sizes: A, 407  $\mu\text{m}^2$ ; B, 264  $\mu\text{m}^2$ ; C, 378  $\mu\text{m}^2$ ; D, 442  $\mu\text{m}^2$ .

III–IV border. To date we have not seen any X-cell axons whose terminal fields completely avoided layer IVa. The terminal arbor of the X-cell contained 3,362 boutons, of which 423 (13%) were in layer IVa, 2,902 (86%) were in layer IVb, and 37 (1%) were in layer VIa.

Surface view outlines and bouton density profiles of the terminal arbor within layer IV were reconstructed as follows: The two-dimensional summary reconstruction shown in Figure 5D was divided into consecutive 100  $\mu\text{m}$  wide sectors by equally spaced lines running through the arbor perpendicular to the layer IV borders. The first sector was arbitrarily started at the left-hand edge of the arbor. The drawing of each consecutive section was then placed in register over the summary drawing, and the number of boutons within each sector in layer IVb was counted. In Figure 7A each successive histogram corresponds to a sin-

gle coronal section through the terminal field in layer IVb and each shows the frequency of boutons per sector. This bouton density profile reveals that the axon terminated within a single, continuous clump in layer IVb. Bouton density was not uniform across the field, but clearly was greatest near the center and decreased significantly toward the edges of the field. The peak of the bouton density in layer IVa, which is not illustrated, matched that in IVb. This center-to-edge gradient in bouton density presumably reflects a similar gradient in synaptic density across the terminal field. Preliminary data for other X-cell arbors suggest that their bouton density profiles were similar to that shown in Figure 7A, but further analysis is necessary to confirm this. Figure 7B illustrates the shape and total area of this X-cell axon's terminal field in layer IVb. Each line plots the lateral extent of boutons within each successive section. At its maximum points, the field extended about 1.2 mm dorsoventrally on the medial bank and about 1.0 mm anteroposteriorly. Its surface area of 0.6  $\text{mm}^2$  represents the total area in layer IVb that potentially received input from the X-cell.

**X-cell projections to layer IVa.** Another X-cell projection pattern that we have observed (four out of 12 X-cell axons) is shown in Figure 8. The location of the axon arbor in area 17 and the relatively small geniculate soma (291  $\mu\text{m}^2$ ) in lamina A are illustrated in Figure 8A–C. Interestingly, when traced back from the injection site (arrow in Fig. 8A) the parent axon coursed dorsally toward the crown of the lateral gyrus and then reversed direction, traveling ventrally again. We have occasionally seen other examples of major changes in the trajectories of axons as they coursed through the white matter. These trajectories may reflect aberrant target finding behavior of the developing axons as they grew into cortex.

Figure 8D illustrates the axon's terminal field in greater detail. While every physiological property of the axon was typical of X-cells (see Fig. 8 legend for details), the axon terminated mainly within layer IVa and in the layer III–IV border region (2,270 boutons, 87%), and had only a minor input to the upper half of layer IVb (140 boutons, 5%). Also, the axon distributed 190 boutons (8%) about equally between layers VIa and VIb. Curiously, the layer VI arbor is not in register with the layer IV arbor above; instead, the layer VI arbor seems shifted to the right side of the field, and has a slightly more eccentric retinotopic location. We have noted this positional disparity in the reconstructions of other X- and Y-cell axons, but we cannot yet rule out the possibility that it is simply an artifact of the plane of cut perhaps not being aligned properly with the cell columns rising through cortex. If this reflects a true misalignment, it may relate to intracortical circuits suggested by Gilbert and Wiesel ('79, '83) by which layer VI cells might provide inhibitory inputs to layer IV simple cells to form the inhibitory end zones or flanks in their receptive fields (e.g., Bishop et al., '71; Sherman et al., '76); these flanks would be slightly offset from the excitatory centers of the receptive fields. Finally, a surface view of the shape and extent of this axon's layer IV arbor is shown in Figure 8E. The arbor was about 0.9 mm wide by 1.5 mm long, it occupied a total area of 0.9  $\text{mm}^2$ , and, like most other X-cell arbors, it terminated in a single, continuous clump.

**X-cell projections throughout layer IV.** A third type of arborization observed in four of 12 X-cell axons is illus-

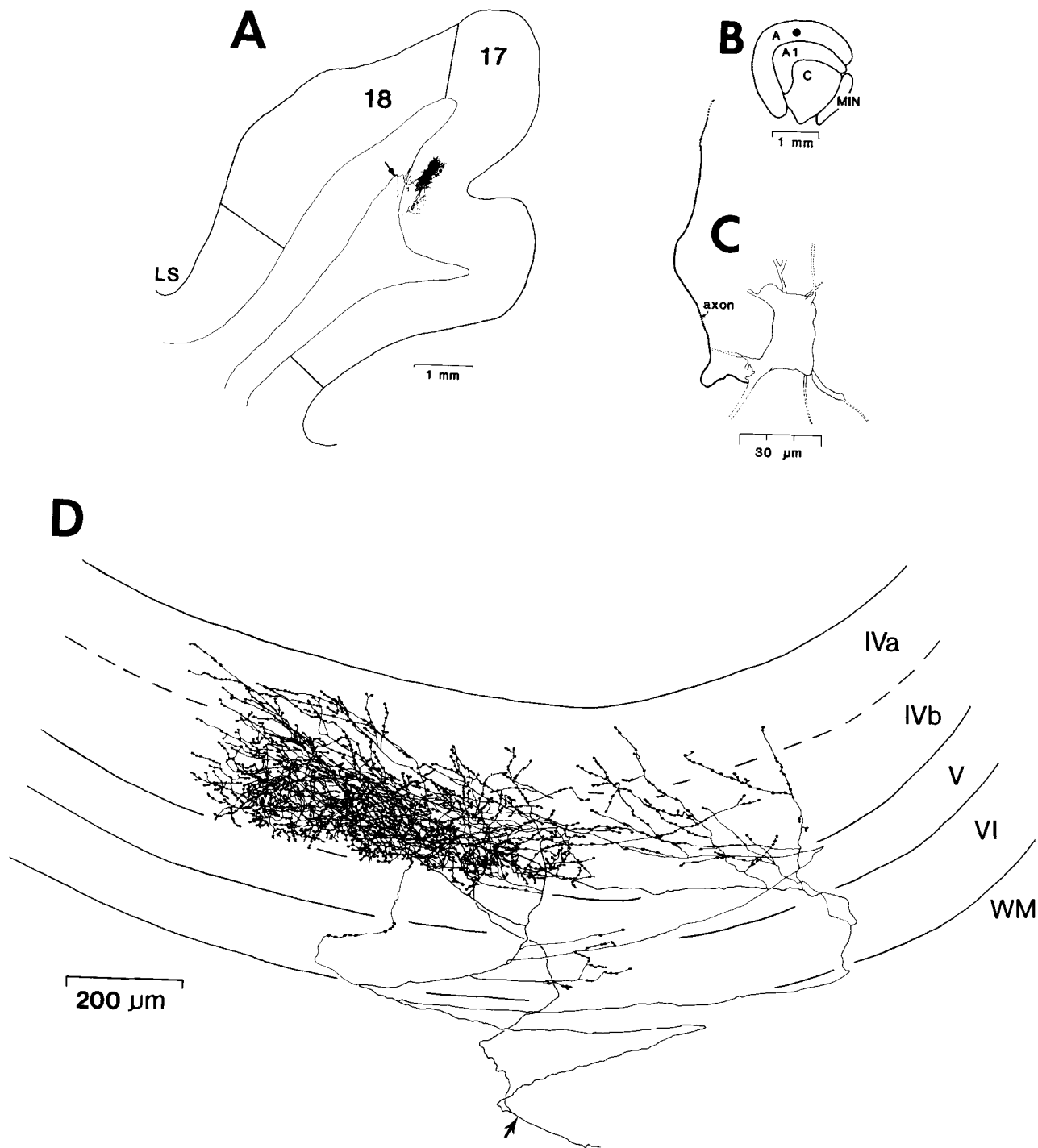


Fig. 5. Reconstruction of an X-cell that projected mainly to layer IVb. The cell had an off-center receptive field,  $1.5^\circ$  in center diameter, that was located  $11^\circ$  from the vertical meridian and  $12^\circ$  below the horizontal zero parallel, and was activated through the contralateral eye. It responded linearly to counterphased sine wave gratings and was activated electrically from the optic chiasm at 3.0 msec. No optic radiation electrodes were used in this animal. A. Lower power reconstruction of the complete terminal field and parent axon, viewed in coronal section. The axon arborized at the base of the suprasplenial sulcus in area 17. Arrow points to the injection site. The diameter of parent axon was  $2.0 \mu\text{m}$ . 17, area 17; 18, area 18; LS, lateral sulcus. B. Outline of the coronal section containing the retrogradely

filled cell in the lateral geniculate nucleus. The filled circle marks the cell's location in the middle of lamina A. C. Reconstruction of the cell. The HRP clearly labeled the cell body ( $407 \mu\text{m}^2$ ), the intrageniculate portion of the axon, and a few proximal dendrites. D. Higher power drawing of the complete axon terminal field reconstructed from ten serial coronal sections. The field has been rotated relative to A, with the pial surface now up. Note the dense plexes of fine, bouton-laden collaterals within layers VI, IVb, and lower IVa. The arrow indicates the injection site. For all of the following X- and Y-cells, the low power reconstructions of the arbors and the outlines of the LGNs and cell bodies are printed at the same scale as those shown here, allowing direct comparison of these features among the reconstructed cells.

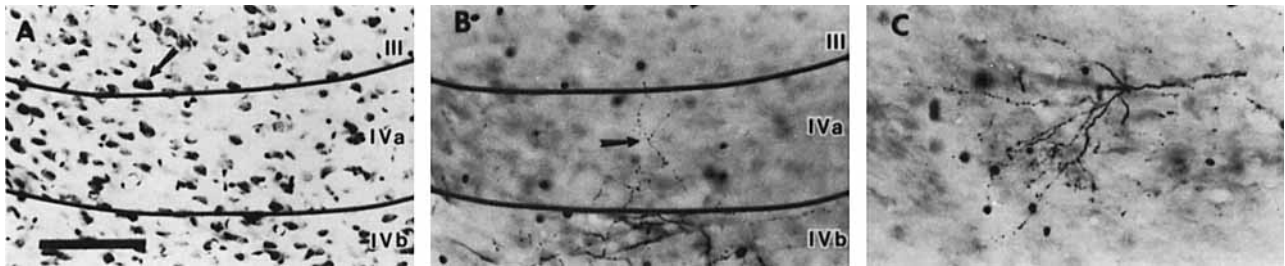


Fig. 6. Photomicrographs of the terminal field of the X-cell axon illustrated in Figure 5D. A. Nissl stained cell bodies and the layer III-IVa and IVa-IVb boundaries. Arrow indicates large pyramid at the base of layer III. Scale bar = 100  $\mu$ m and applies to B and C. B. Terminal processes in the same field of view as in A, but deeper in the section. A deep blue filter (Wratten 48A) was used to enhance contrast of the HRP-filled processes and

reduce contrast in the Nissl stained cell bodies. Note the terminal process (arrow) rising vertically through layer IVa and crossing the layer III-IV border. The actual height of this process is not apparent in the reconstruction in Figure 5D, due to minor distortion in the reconstruction. C. Fine terminal processes visible in another portion of the arbor. These largely occupy layer IVb.

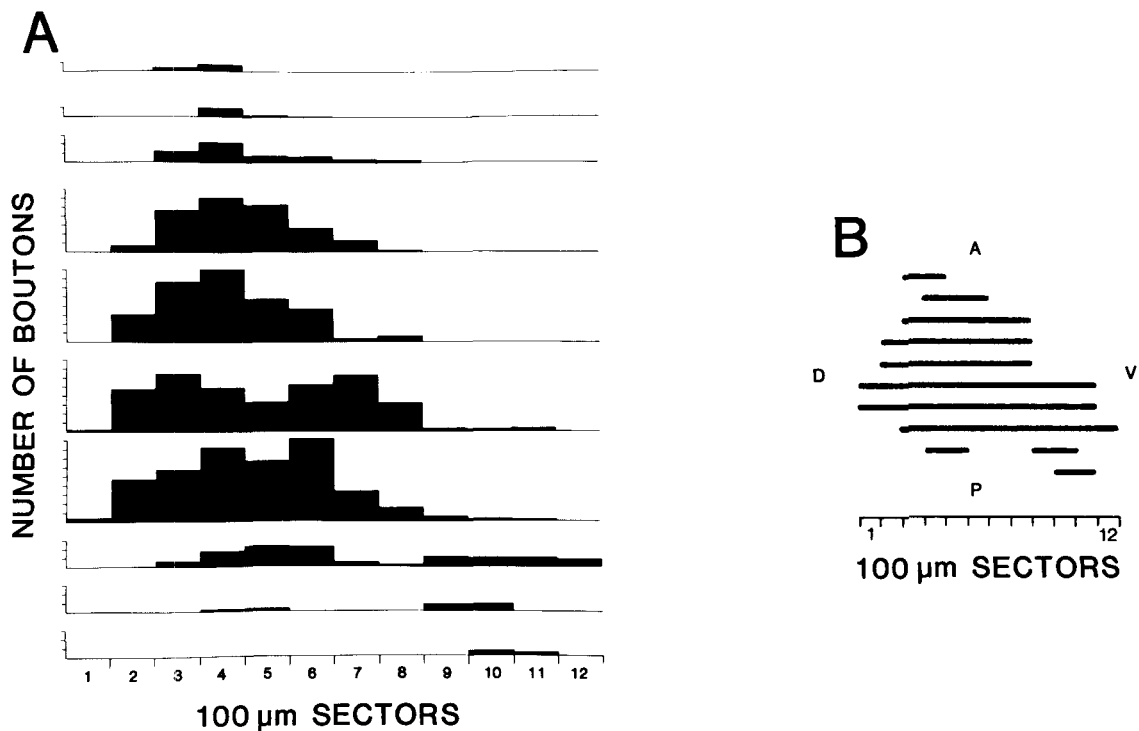


Fig. 7. Bouton density profile and surface view outline of the X-cell axon shown in Figure 5D. A. Bouton density profile. Each histogram plots the number and spatial distribution of boutons within each coronal section through the terminal field in layer IVb. Each mark on the Y-axis denotes 20 boutons. See text for further description. B. Surface view outline derived from the bouton density profile. In this, and in subsequent surface views,

each line corresponds to a single coronal section through the terminal arbor. Its extent indicates those sectors that contain one or more boutons. A, anterior; P, posterior; D, dorsal (toward the apex of the gyrus); V, ventral (toward the splenic sulcus). All surface view outlines in subsequent reconstructions are matched to scale with this one, allowing direct comparison of the shapes and extents of X- and Y-cell terminal arbors.

Fig. 8. Reconstruction of an X-cell axon that projected mainly to layer IVa. The cell had a receptive field with a tonic on-center,  $0.6^\circ$  in diameter, that was located  $6^\circ$  from the vertical meridian and  $1^\circ$  above the horizontal zero parallel. It was activated through the contralateral eye, it responded linearly to counterphased gratings, and it responded poorly to a rapidly moving disk. Its (OX - OR) latency was 2.0 msec. A. Lower power reconstruction of the terminal field and parent axon. The arrow points to the injection site, and the diameter of the parent axon was 1.5  $\mu$ m. B. Lower

power drawing of the lateral geniculate nucleus. The filled circle in the ventral third of lamina A marks the location of the cell body. C. Higher power drawing of the retrogradely filled cell body (291  $\mu$ m<sup>2</sup>) and primary dendrites. D. Higher power drawing of the complete axon terminal field reconstructed from 15 serial sections. The axon terminated throughout layers VI, IVa, and the III-IV border zone and largely avoided layer IVb. E. Surface view of the shape and extent of the terminal field in layer IV. Conventions as in Figures 5 and 7.

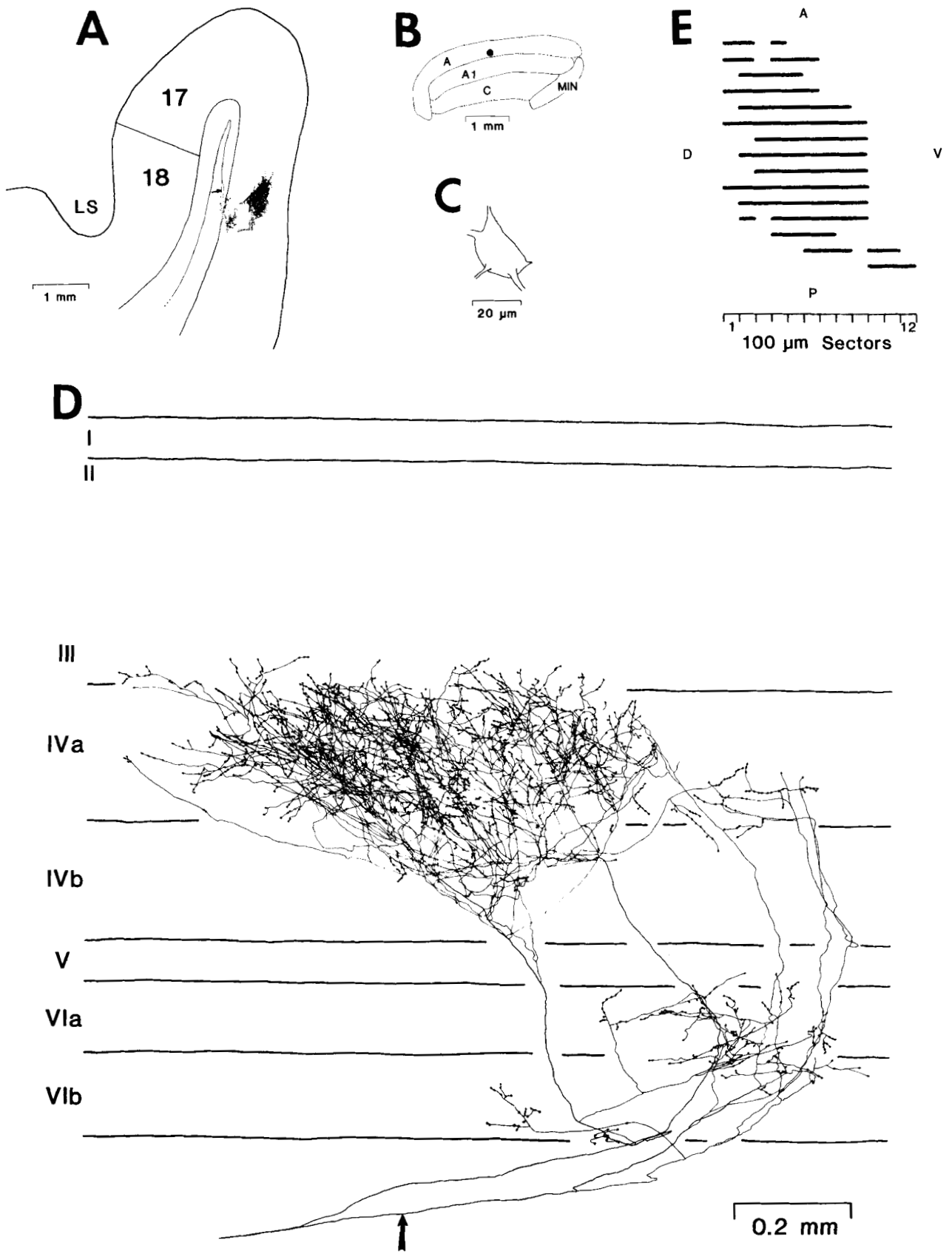


Figure 8

trated in Figure 9. The axon arose from a relatively small ( $281 \mu\text{m}^2$ ) soma in the upper one-third of lamina A of the LGN and projected to the medial bank of area 17 (Fig. 9A-C), where it arborized densely. Single sections through the terminal field (Fig. 9D) reveal its terminals in the upper two-thirds of layer VI (419 boutons, 9%), throughout layer IVb (1,310 boutons, 27%), and throughout layer IVa (2,382 boutons, 49%). It also terminated (735 boutons, 15%) up to  $100 \mu\text{m}$  into lower layer III. Examples of these boutons are shown in the photomicrographs of Figure 10. Strings of bouton-laden processes clearly rose through layer IVb and IVa and intermingled with the cell bodies of the large border pyramids at the base of layer III. Thus, visual information conveyed by this axon was potentially capable of directly (i.e., monosynaptically) reaching cells throughout layer IV as well as the lower portions of layer III. It is interesting that, although the axon arborized throughout layer IV, it terminated twice as densely in layer IVa as in layer IVb. Finally, a few (17, <1%) boutons were scattered within layer Va and layer Vb.

A surface view outline of this axon's terminal field in layer IV is illustrated in Figure 9E. As with most other X-cells, the axon arborized in a single clump. Its surface area was  $0.7 \text{ mm}^2$ . Although the axon arborized through a number of layers in area 17, its lateral extent was no greater than most other X-cell axons terminating there.

Another example of an X-cell arborizing throughout layer IV is shown in Figure 11. The axon originated from a soma ( $338 \mu\text{m}^2$ ) in the lower one-third of lamina A1, and it arborized in cortex along the dorsal lip of the splenial gyrus (Fig. 11A-C). Here it terminated extensively throughout layer IVb (325 boutons, 27%), layer IVa (533 boutons, 44%), and deep layer III (96 boutons, 8%) within  $100 \mu\text{m}$  of the III-IV border (Fig. 11D). Thus, while the axon showed no sublaminal restriction in its termination in and around layer IV it terminated most densely in layer IVa and III. As well, there was a sizable input into layer VI (271 boutons, 21%), primarily to the upper half. The surface view of this axon (Fig. 11E) reveals that the arbor formed a long (1.5 mm) and narrow (0.3 to 0.4 mm) continuous zone,  $0.6 \text{ mm}^2$  in area, that ran generally in an anteroposterior direction along the gyral lip. Presumably the arbor was aligned along a single ocular dominance column representing the ipsilateral eye.

We have been surprised by the number of X-cell axons (one-third of our sample) that arborized extensively throughout both divisions of layer IV. Such projection patterns appear to be common among X-cells throughout the central  $30^\circ$  of the visual field representation in cortex. Figure 12 shows another reconstruction of an arbor from an X-cell whose soma ( $323 \mu\text{m}^2$ ) was located in the ventral third of lamina A (Fig. 12B,C). The axon terminated in layer VIa (35 boutons, 2%), in layer IVb (684 boutons, 42%), in layer IVa (892 boutons, 54%), and along the layer III-IV border zone (24 boutons, 1%) (Fig. 12A). In addition, a few bouton-laden collaterals (ten boutons, 1%) dipped into layer Va. The shape and extent of this axon's terminal arbor in layer IV are shown in the surface view outline in Figure 12D. The arbor's dimensions were roughly 0.9 by 1.5 mm, occupying a total area of  $0.8 \text{ mm}^2$ .

### Y-cell projections to area 17

The laminar projections of Y-cells to area 17 were somewhat less variable than were those of X-cells. Five of the seven reconstructed Y-cell axons that projected to area 17 ended almost exclusively in the upper half of layer IV and

lower layer III. However, two contributed significant numbers of boutons to the lower half of layer IV as well.

**Y-cell projections to layer IVa.** One Y-cell axon projection pattern is illustrated in Figure 13. The axon arose from a cell body ( $380 \mu\text{m}^2$ ) in the dorsal third of lamina A1 (Fig. 13B,C). The axon terminated in layer VIb (336 boutons, 16%) and layer VIa (212 boutons, 10%), and distributed a few (12, <1%) boutons in layer Va & b (Fig. 13D). It then arborized in two separate clumps in layer IVa (1,251 boutons, 59%) and in the lower  $200 \mu\text{m}$  of layer III (269 boutons, 13%). Figure 14 illustrates some of the boutons in layer III. About 34 boutons (2%) also were distributed to layer IVb. A number of these were contributed by a small collateral which formed a third "clump" on the left side of the field. Note that the main arbors in layer VI and layer IV were apparently shifted out of retinotopic alignment, as was the case for one of the X-cell arbors noted above (Fig. 8D).

The surface view (Fig. 13E) of the Y-cell's terminal arbor in layer IV reveals three separate terminal regions formed by the two main arbors in layer IVa plus the small collateral that projected mainly to layer IVb. The two main arbors were separated by a terminal-free gap of about  $600 \mu\text{m}$ . The total extent of the layer IV field, including all gaps, was about 1.6 by 2.0 mm, covering a total area of about  $1.1 \text{ mm}^2$ . This is about 1.4 times the extent of an average X-cell arbor. However, when one subtracts the gaps between the clumps of boutons, the area of the actual layer IV terminal arbor itself was about  $0.7 \text{ mm}^2$ , and is on the order of that seen among many X-cells. The clumping nature of the terminal arbor of this Y-cell may reflect the axon's divergence into two or three adjacent ocular dominance columns representing the ipsilateral eye, with the gaps corresponding to the sites of afferents from the contralateral eye. The width of the main terminal-free gap ( $600 \mu\text{m}$ ) is similar to that reported for eye dominance columns in the cat (Shatz et al., '77). However, we have not yet directly labeled the ocular dominance columns in our animals and so cannot say how precisely the terminal arbors of X- and Y-cell axons are aligned within the columns. While this has been demonstrated for one geniculostriate axon in the monkey (Blasdel and Lund, '83) it remains to be demonstrated in the cat.

Another example of a Y-cell projection to area 17 is illustrated in Figure 15. The cell's medium-sized soma ( $417 \mu\text{m}^2$ ) was located in the dorsal third of lamina A (Fig. 15B,C). We injected its axon in a primary collateral about 2 mm distal to the first bifurcation point, which occurred deeper in the white matter (Fig. 15A). The terminal arbor from this collateral was well labeled but the other primary collateral

---

Fig. 9. Reconstruction of an X-cell that projected throughout layer IV. The cell had an off-center receptive field,  $0.8^\circ$  in center diameter, that was activated through the contralateral eye and was located  $15^\circ$  from the vertical meridian and  $4^\circ$  below the horizontal zero parallel. It responded linearly to gratings, discharged briskly to a rapidly moving disk, and had (OX - OR) latency of 2.2 msec. A. Lower power reconstruction of the terminal field, parent axon, and injection site (arrow). The parent axon diameter was  $1.0 \mu\text{m}$ . B, C. Drawing of the retrogradely filled cell, located in the dorsal third of lamina A (filled circle) of the lateral geniculate nucleus. The soma size was  $281 \mu\text{m}^2$ . D. Higher power reconstructions of the terminal arbor in four sections through the terminal field. Section numbers are indicated in parentheses. Note the dense terminations within layers VI, IV, and lower III. E. Surface view of the shape of the layer IV terminal field. Conventions as in Figures 5 and 7.

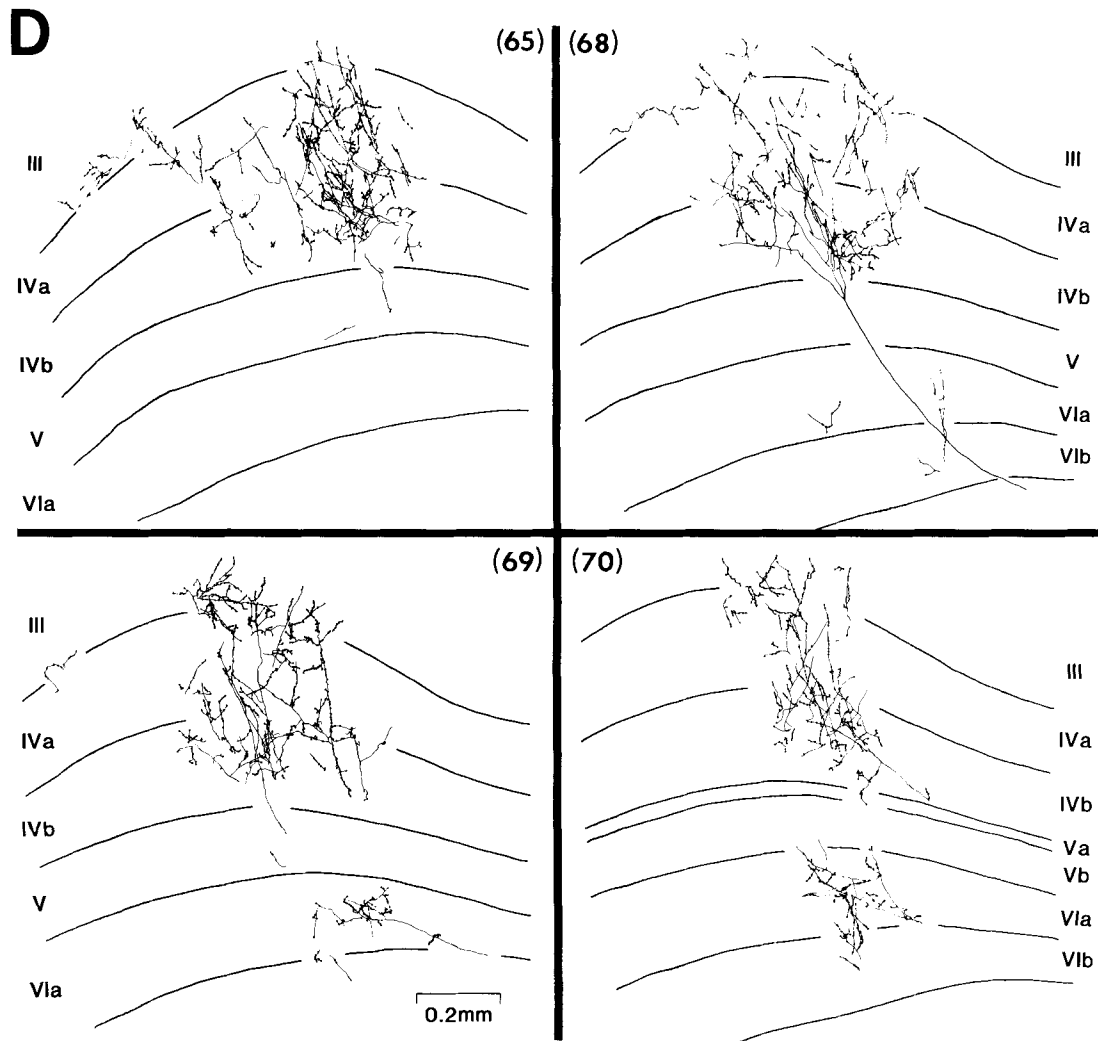
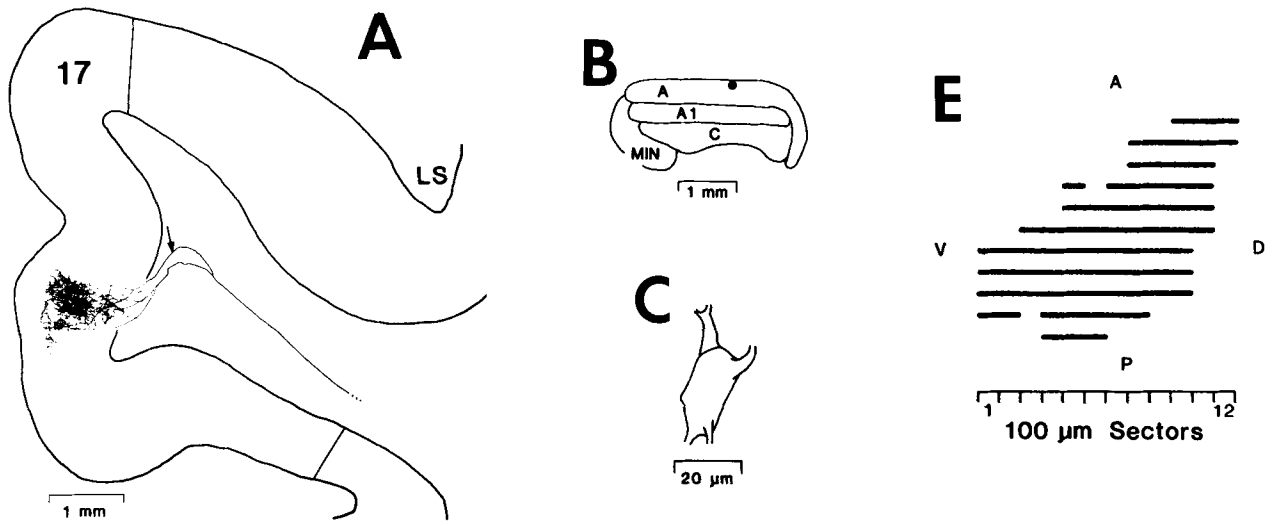


Figure 9

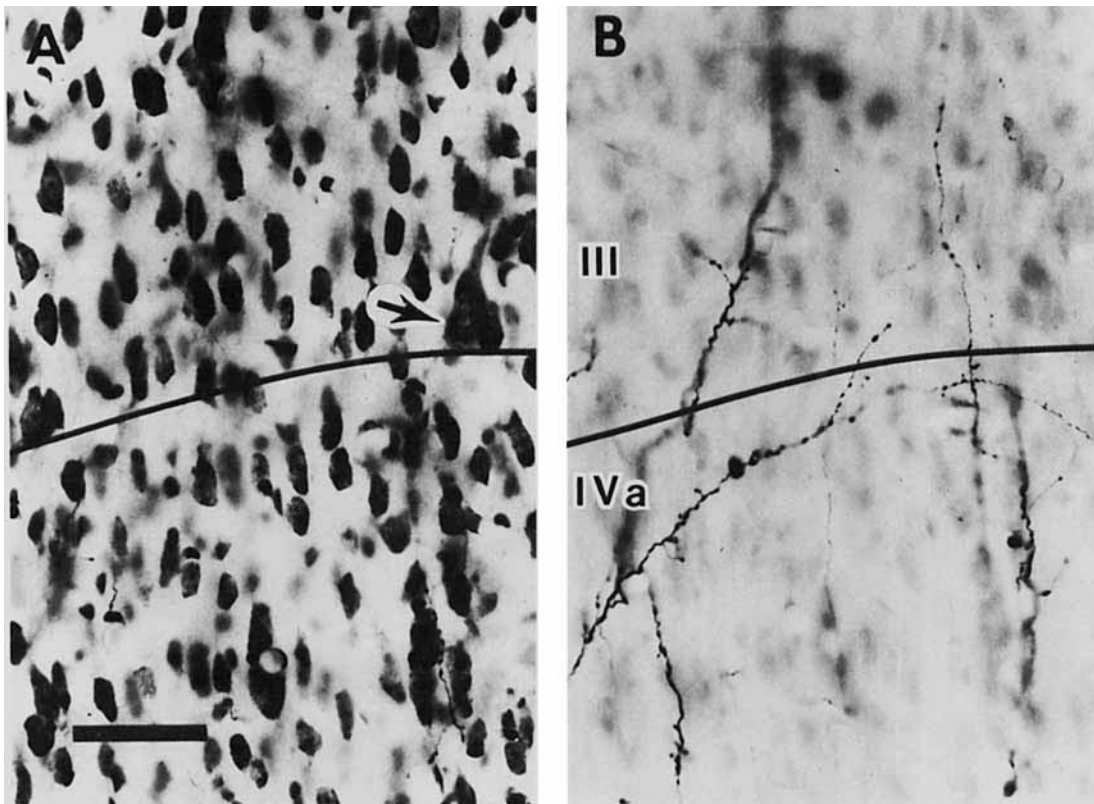


Fig. 10. Photomicrographs of the boutons from the X-cell axon shown in Figure 9. A. Nissl stained cell bodies in layers III and IVa. The arrow points to a large pyramid at the base of layer III. Scale bar = 50  $\mu\text{m}$  and applies to B. B. Terminal processes at a deeper plane of focus in the same field of view as A. A blue filter was used for photography (see legend to Fig. 6B). Note the processes in layer IVa and lower layer III.

was too poorly labeled to visualize its arbor. Such incomplete filling was generally a greater problem among Y-cell axons than among X-cell axons, because some Y-cell axons (and few X-cell axons) initially bifurcated in the white matter 2 to 4 mm from their terminal arbor. The resulting collaterals themselves may bifurcate further before entering cortex. If one injects a collateral more than 2 mm distal to the first bifurcation, its portion of the terminal arbor may be well filled but other portions may not be, due to the great distances over which the HRP must be transported. This occurred for the axon shown in Figure 15A. Despite this problem, the well-labeled portion of the terminal arbor provided useful information regarding the axon's laminar projections. We have found among most X- and Y-cell axons that each of the two primary collaterals emanating from a cell's parent axon generally projected to the same laminae, and even sublaminae, within visual cortex.

Reconstructions of three consecutive sections through this field are illustrated in Figure 15D. Like other Y-cell axons, this terminated primarily in layer IVa, along the layer III-IV border zone (2,800 boutons, 74%), and in both divisions of layer VI (950 boutons, 25%). A small number of boutons (27, 1%) also were present in the top of layer IVb. When viewed from the surface (Fig. 15E), the arbor in layer IV was about 1.3 mm long and from 0.3 to 1.3 mm wide, with a total surface area of 0.9  $\text{mm}^2$ . The length and surface

area probably are overestimated somewhat since there is some vertical distortion in the two dimensional summary reconstruction of this field (Fig. 15A). Examination of the individual sections indicates that there may have been three major clumps of boutons across the arbor (not illustrated), though they do not appear nearly as segregated from one another as the Y-cell arbor shown in Figure 13.

**Y-cell projections throughout layer IV.** We have observed two Y-cell axons out of the seven analyzed in detail that arborized densely throughout the depth of layer IV. One such axon is illustrated in Figure 16. It arose from a large cell body (497  $\mu\text{m}^2$ ) that was located in the middle third of the depth of lamina A (Fig. 16B,C), and it gave rise to a large and prolific (6,669 boutons) terminal arbor deep in the medial bank of area 17 (Fig. 16A). The cell's main input was to layer IVa (4,017 boutons, 60%) but it also terminated densely throughout the depth of layer IVb (1,702 boutons, 26%). Other terminals were distributed throughout layers VI (605 boutons, 9%), V (68 boutons, 1%), and lower layer III (277 boutons, 4%). Thus, some Y-cells contribute significantly to layer IVb. We do not believe that the layer IVb input for this axon simply reflects an overall breakdown in sublaminal segregation among those Y-cells that represent more peripheral regions of the visual field. The axon illustrated in Figure 15 provided practically no boutons to layer IVb, even though its receptive field was

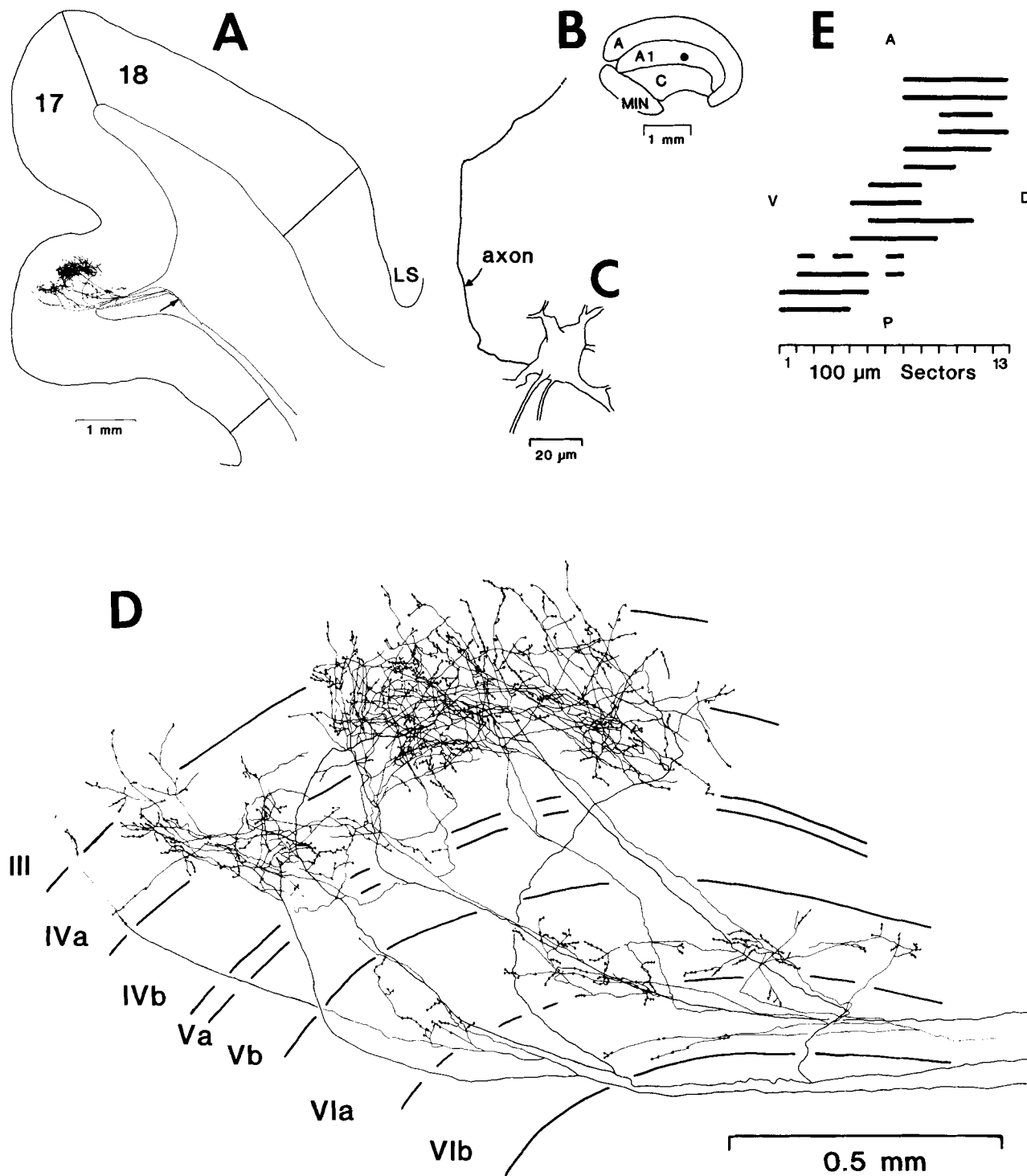


Fig. 11. Reconstruction of another X-cell axon that projected throughout the depth of layer IV. The cell's off-center receptive field,  $0.8^\circ$  in center diameter, was driven through the ipsilateral eye and was located  $19^\circ$  from the vertical meridian and  $18^\circ$  below the horizontal zero parallel. It responded linearly to counterphased gratings and poorly to a fast moving disk, and it was activated from the optic chiasm with a latency of 2.0 msec. A. Lower power drawing of the terminal field and parent axon. The injection

site is indicated by an arrow, and the diameter of the parent axon was  $1.5 \mu\text{m}$ . B, C. Drawing of the lateral geniculate nucleus and retrogradely filled cell body ( $338 \mu\text{m}^2$ ) that was located in the lower portion of lamina A1. D. Higher power drawing of the full terminal arbor reconstructed from 14 serial sections. The axon terminated throughout layers VI, IV, and lower layer III. E. Surface view of the shape and extent of the layer IV terminal field. Conventions as in Figs. 5 and 7.

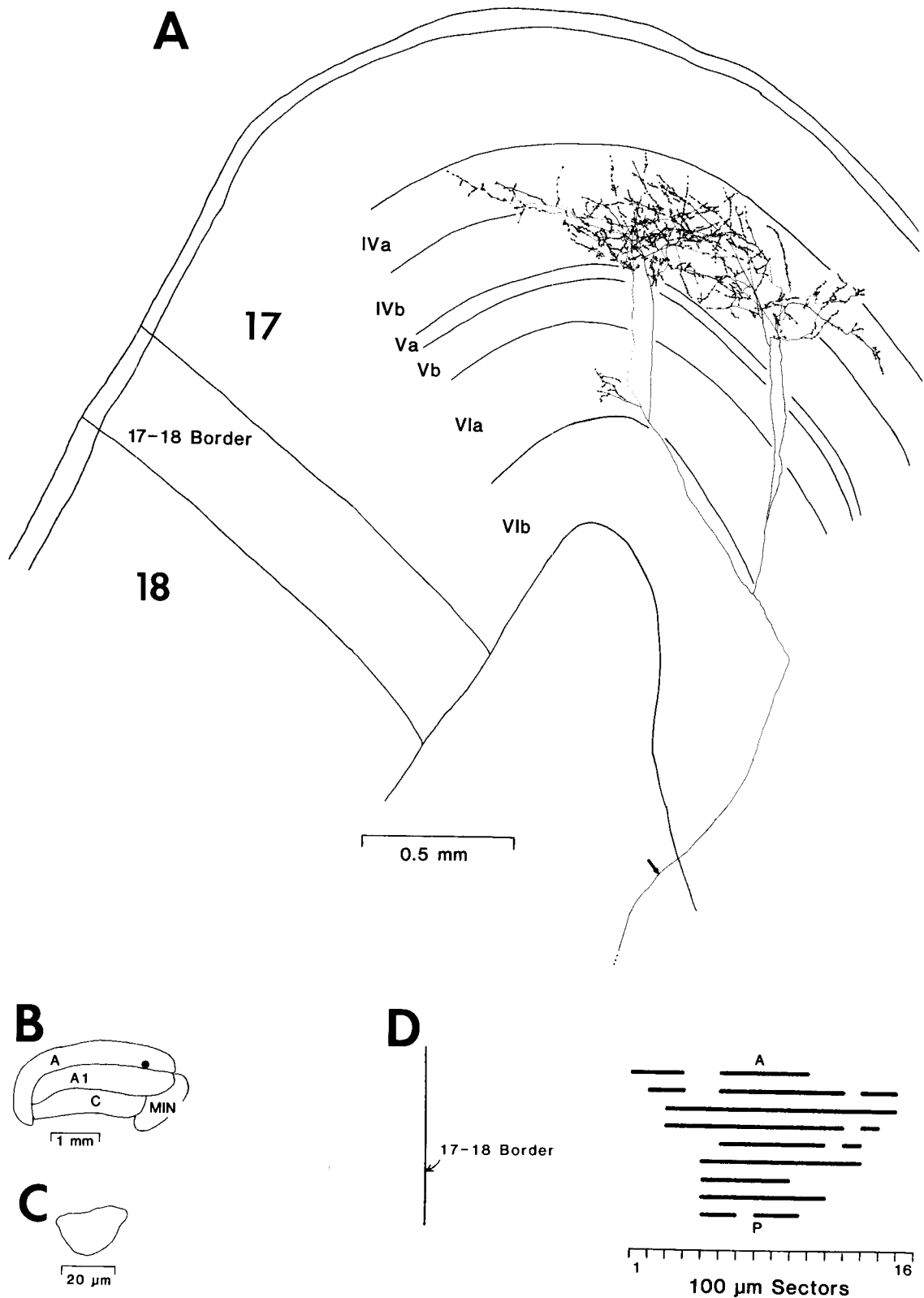


Fig. 12. Reconstruction of an X-cell axon that projected throughout layer IV. The cell had an on-center receptive field,  $0.5^\circ$  in center diameter, that was driven through the contralateral eye and was located  $3^\circ$  from the vertical meridian and  $10^\circ$  below the horizontal zero parallel. It summed linearly, responded poorly to a fast moving disk, and had an (OX-OR) latency of 1.5 msec. A. Drawing of the complete terminal arbor reconstructed from nine serial sections. The arrow marks the point of injection,

and the axon diameter was  $1.5 \mu\text{m}$ . B, C. Drawing of the lateral geniculate nucleus, location of the retrogradely filled cell body (filled circle) and outline of the cell soma. The soma was lightly labeled with HRP making it difficult to clearly distinguish its outline. Its estimated surface area was  $323 \mu\text{m}^2$ . D. Surface view outline of the layer IV terminal field, and its location relative to the 17-18 border. Conventions as in Figures 5 and 7.

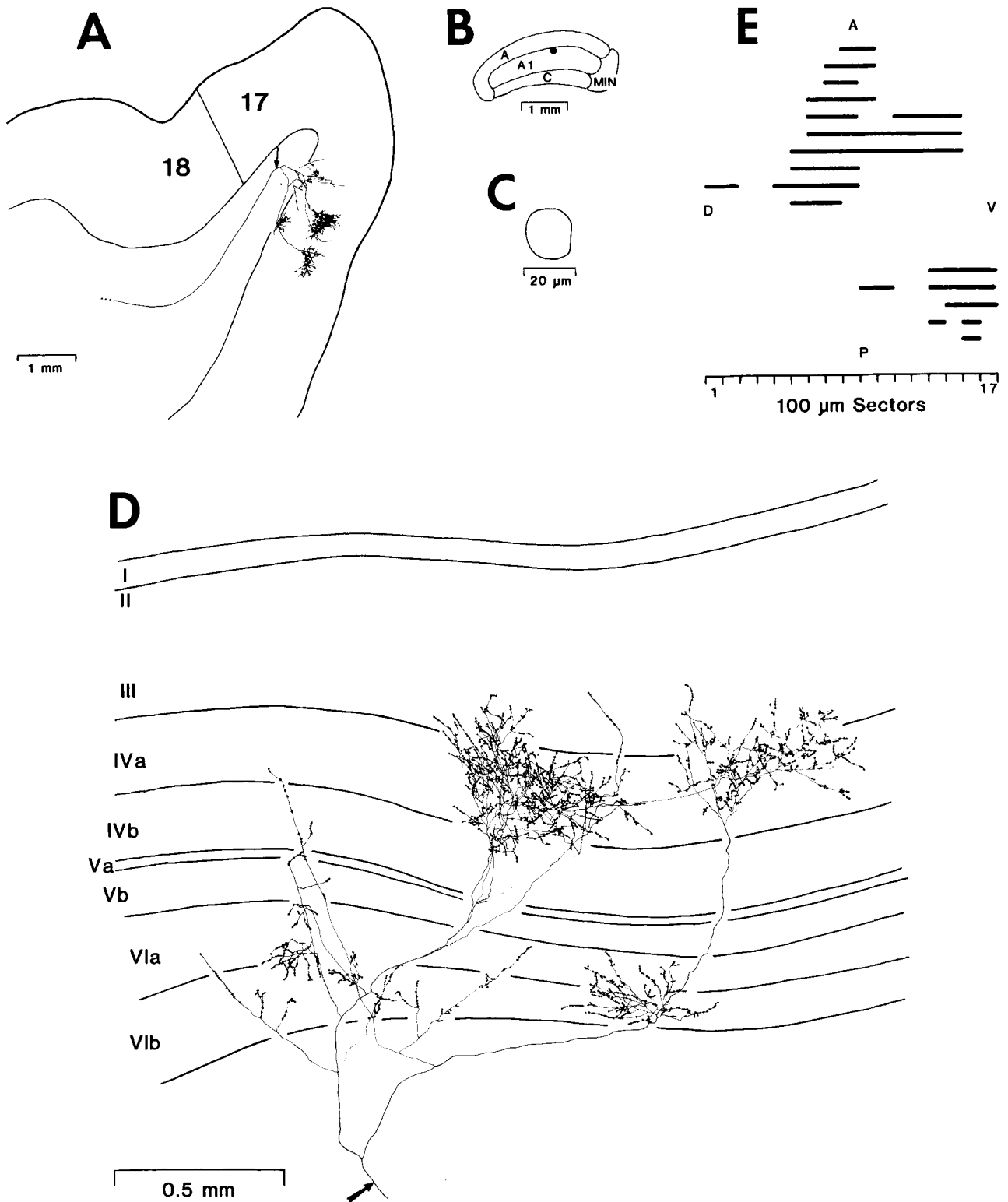


Fig. 13. Reconstruction of a Y-cell that projected mainly to layer IVa. The cell's on-center receptive field,  $0.5^\circ$  in center diameter, was driven through the ipsilateral eye and was located  $7^\circ$  from the vertical meridian and  $7^\circ$  below the horizontal zero parallel. The cell responded nonlinearly to gratings, responded well to a fast moving disk, and had an (OX-OR) latency of 1.6 msec. A. Lower power drawing of the terminal arbor. The arrow points to the injection site, and the parent axon diameter was  $2.0 \mu\text{m}$ . B,C. Drawing of the lateral geniculate nucleus showing the location of the

backfilled cell (filled circle) in lamina A1, and an outline of the cell soma ( $380 \mu\text{m}^2$ ). D. Higher power detailed drawing of the laminal projections of the cell, reconstructed from 15 serial sections. The axon terminated densely throughout layers VI, IVa, and lower layer III, and very sparsely in layers IVb and V. Note the separate clumps of boutons in both layers VI and IV. The arrow points to site of injection. E. Surface view outline of the shape, extent, and clumping nature of the layer IV terminal field. Conventions as in Figures 5 and 7.

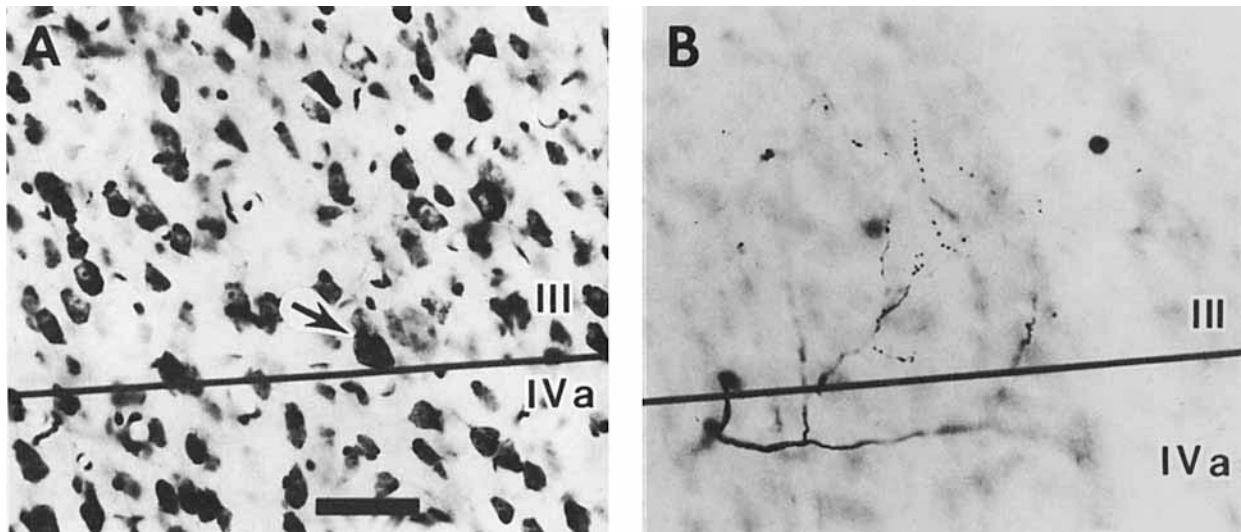


Fig. 14. Photomicrographs showing the laminar location of some terminal processes in the Y-cell arbor illustrated in Figure 13D. A. Nissl stained cell bodies in upper layer IVa and lower layer III. The arrow points to a large pyramid at the base of layer III. Scale bar = 50  $\mu\text{m}$  and applies to B. B. Terminal processes in layer III. This is the same field of view as in A, and was photographed with a blue filter (see legend to Fig. 6B).

even more eccentric than that in Figure 16. Also, the other Y-cell axon that arborized throughout layer IVa and IVb (not illustrated) had a receptive field located only  $10^\circ$  from the vertical meridian.

#### Summary of X- and Y-cell projection patterns

A number of features are common to most of the X-cell terminal fields observed so far. All of the axons terminated in area 17. They arborized mainly in layers VI and IV, but some also terminated in lower layer III and/or layer V. The layer V input was seen in four of the 12 reconstructed X-cells but generally accounted for much less than 1% of each axon's boutons. The layer IV arbor generally consisted of a single, continuous zone of boutons, covering a surface area of 0.6 to 0.9  $\text{mm}^2$  (Fig. 17). Each zone may occupy a single ocular dominance column. However, one of the reconstructed X-cell axons (not illustrated) arborized over a wider region of about 1.4  $\text{mm}^2$  and formed three to four separate clumps (in layer IVa) separated by terminal free gaps about 300 to 500  $\mu\text{m}$  wide.

The terminal arbors of X-cells differed from one another in three major ways, the main one being their projection within layer IV. Some cells terminated mainly in layer IVb (four of 12), others mainly in layer IVa (four of 12), and still others throughout both divisions of layer IV (four of 12). The latter two groups always distributed across the layer III-IV border and up to 100  $\mu\text{m}$  into layer III. A second difference was found among X-cell projections into layer VI. As a group, X-cells projected throughout the depth of layer VI, although the projection was heaviest in the upper half. Among cells, however, there was a significant variation in both the density and sublaminar locations of the layer VI input. The number of terminals in layer VI varied from 35 to 419, with an average of 220; this represented a range of 1% to 22%, with an average of 10%, of each axon's total boutons. Within this range, some axons terminated only in layer VIa (e.g., Fig. 12A) while others arborized throughout

the layer (e.g., Fig. 8A). These differences in layer VI projections were not obviously related to the differences in sublaminar projection patterns in layer IV or to any other anatomical or physiological parameters we have investigated so far. The third major difference among X-cell axons was the variation in the total numbers of boutons in their terminal fields. These ranged from roughly 1,000 to 4,800 with an average of 2,620 (Fig. 18).

As noted above, Y-cell axons were somewhat less heterogeneous in their laminar projection patterns than were X-cell axons. The main input of all seven Y-cells was to layer IVa and lower layer III. The axons terminated as high as 200  $\mu\text{m}$  into layer III, somewhat higher than did the X-cell axons. Two Y-cell axons terminated densely within layer IVb as well as within layer IVa. Thus, some Y-cell input reached all levels of layer IV. All Y-cell axons had a variable input to layer VI, with some terminating in layer VIa and others throughout layers VIa and VIb. The number of boutons distributed to layer VI varied from 67 to 970 with

Fig. 15. Reconstruction of another Y-cell that projected mainly to layer IVa. The cell had an on-center receptive field,  $5^\circ$  in center diameter, that was driven through the contralateral eye and was located  $37^\circ$  from the vertical meridian and  $26^\circ$  below the horizontal zero parallel. It responded nonlinearly to gratings and had a 2.6 msec latency to OX stimulation. No optic radiation electrodes were used. A. Lower power drawing of the terminal arbor, parent axon, and injection site (arrow) in one of the primary axon collaterals. The diameter of parent axon was 2.5  $\mu\text{m}$ . B,C. Drawing of the lateral geniculate nucleus showing the location (filled circle) of the retrogradely filled cell body (417  $\mu\text{m}^2$ ) in lamina A and the extent of the dendritic and axonal filling. The stout, primary dendrites are characteristic of geniculate cells that have a class 1 morphology (Guillery '66) and Y-cell physiological properties (Friedlander et al., '81). D. Reconstructions of the terminal arbor in three consecutive sections. The axon arborized mainly in layers VI and IVa and along the III-IV border zone. E. Surface view outline of the region covered by the arbor in layer IV. Conventions as in Figures 5 and 7.

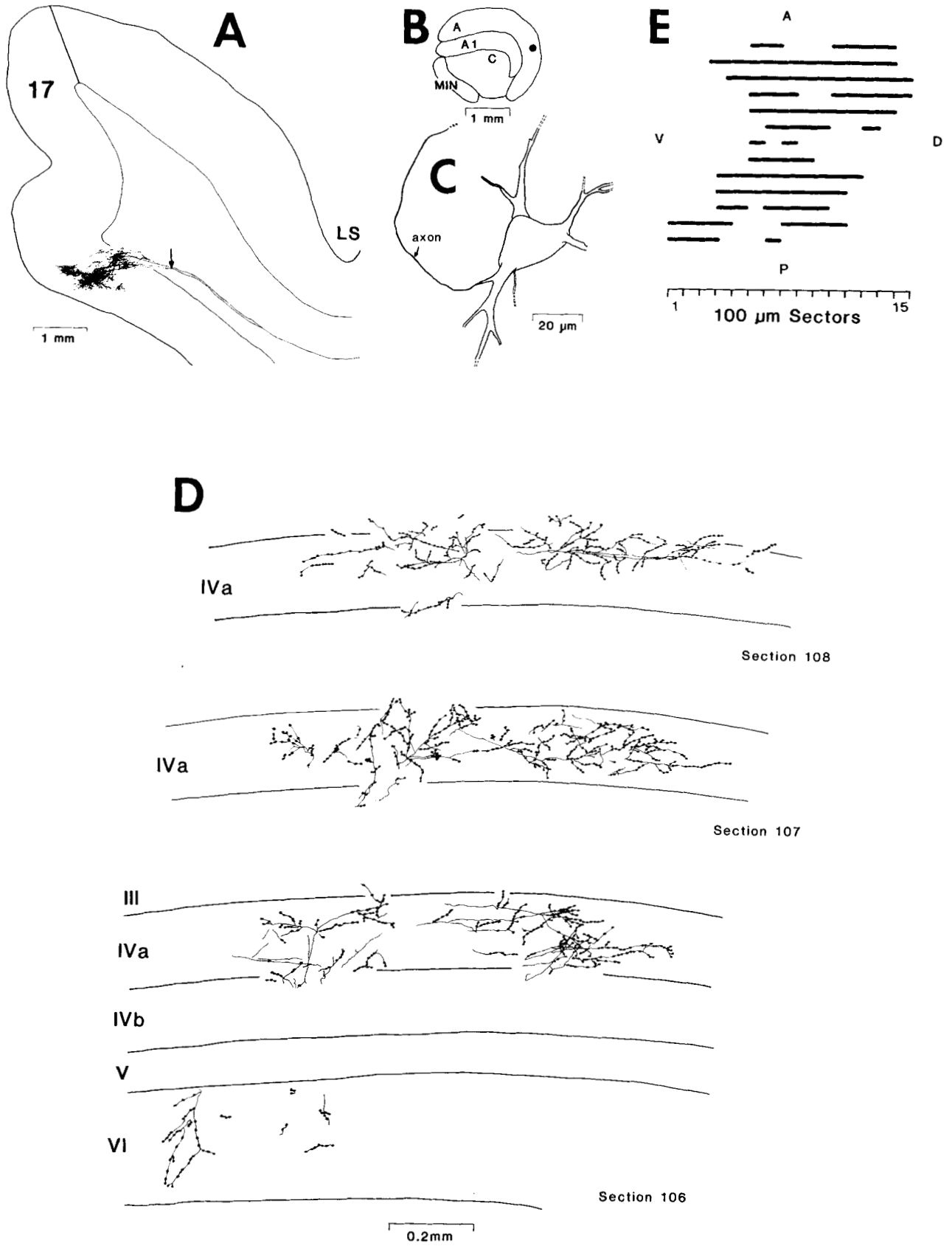


Figure 15

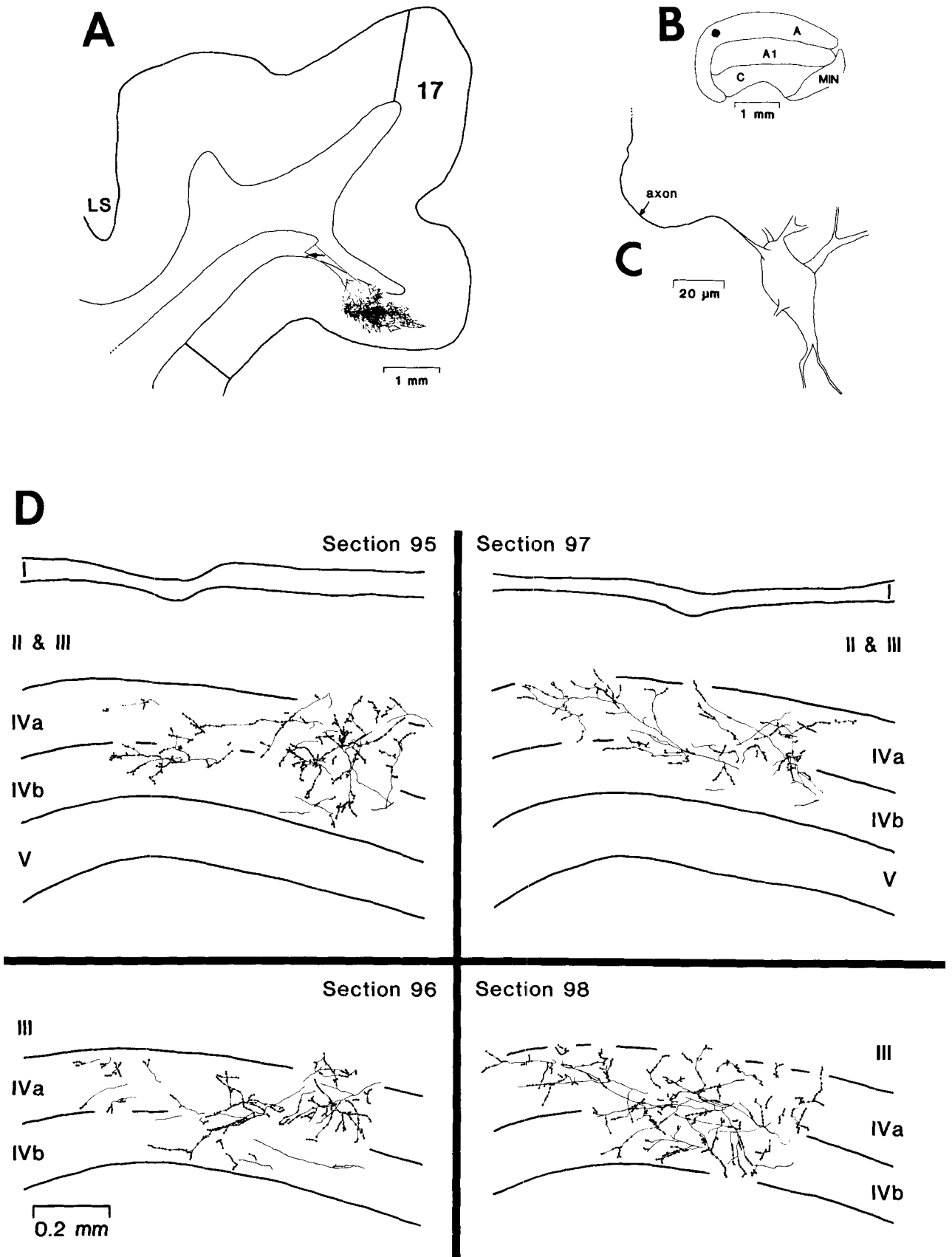


Figure 16

an average of 577, or 1% to 26% with an average of 14% of each axon's total boutons. Single Y-cell axons distributed a significantly greater number of boutons to layer VI than did X-cell axons ( $P < .02$ ), though the percentage of boutons relative to the total numbers is not significantly different for the two groups. As is the case for X-cells, variability in the layer VI projection of Y-cells is not obviously related to any structural or functional parameters we have investigated. Some Y-cells (four out of seven) also distributed a few boutons (four to 68, with an average of 28) into layer V, accounting for 1% or less of their total boutons. The total number of boutons per Y-cell axon within area 17 (Fig. 18) varied from about 2,100 to 6,700 with an average of 4,280 and was significantly greater than that for X-cells ( $P = .03$ ). However, because of the greater chance of not completely filling the Y-cell arbors relative to the X-cell arbors, and the observation that some Y-cell (but not X-cell) axons branch to innervate area 18, we may have underestimated this difference between X- and Y-cell arbors.

The layer IV arbors of Y-cells consisted of one to three major clumps of boutons. When several clumps were present, they were separated by terminal-free gaps of about 500  $\mu\text{m}$ . This is in agreement with the observations of Ferster and LeVay ('78) and Gilbert and Wiesel ('83). The arbors had surface areas (not including gaps) of 1.0 to 1.8  $\text{mm}^2$  with an average of 1.3  $\text{mm}^2$ . This is summarized in Figure 17. Arbors of Y-cells occupied significantly more surface area than those of X-cells ( $P = .004$ ), both when the gaps were included in the measure and when they were not included ( $P = .021$ ).

#### Axon diameters of X-and Y-cells

The diameters of injected X-and Y-cell axons that projected to area 17 are shown in Figure 19A,B. For comparison, we also include the Y-cell axons that terminated in area 18 or that branched to innervate areas 17 and 18. The latter two groups will be presented in more detail in the following paper (Humphrey et al., '85). For all cells shown in Figure 19A, there is a significant relationship between soma size and axon diameter ( $r = .58$ ,  $P < .01$ ). This correlation holds for the subpopulation of X-cells ( $r = .58$ ,  $P < .05$ ) but not for the Y-cells ( $r = .3$ ,  $P > .1$ ). Friedlander et al. ('81) observed a significant relationship between soma size and axon diameter among both cell classes injected in the LGN. Our failure to replicate this for the Y-cell axons may partly reflect the difficulty in densely labeling some Y-cell parent axons which, as noted above, are often located deeper in the white matter than are most X-cell parent axons.

As shown in Figure 19A, Y-cells generally had larger axons than did X-cells, either when all cells are considered ( $P < .001$ ), or when those projecting to area 17 are considered ( $P < .01$ ). However, considerable overlap exists between the two classes in the diameter range of 1.5 to 2.0  $\mu\text{m}$ , and within this range axon diameter is a poor predictor of a geniculate cell's physiological class. Among X- and Y-cell axons, we found no relationship between axon diameter and sublamina of termination within layer IV. X-cell axons that projected mainly to layer IVa had diameters of 1.0 to 1.5  $\mu\text{m}$  (Fig. 19B); those that innervated layer IVb were 1.5 to 2.0  $\mu\text{m}$  in diameter but were not significantly larger than those projecting to layer IVa. Among Y-cells, axon diameter was not related to sublaminar projection (Fig. 19B;  $r = .49$ ,  $P > .1$ ) possibly because all Y-cell axons projected mainly to layer IVa. Finally, as expected, geniculate X- and Y-cells with thicker axons exhibited shorter (OX-OR) latency differences than cells with thinner axons ( $r = .71$ ,  $P < .01$ ).

#### Soma sizes of X- and Y-cells

The soma sizes of 44 retrogradely filled X-cells located in the A-laminae are illustrated in Figure 20A. With two

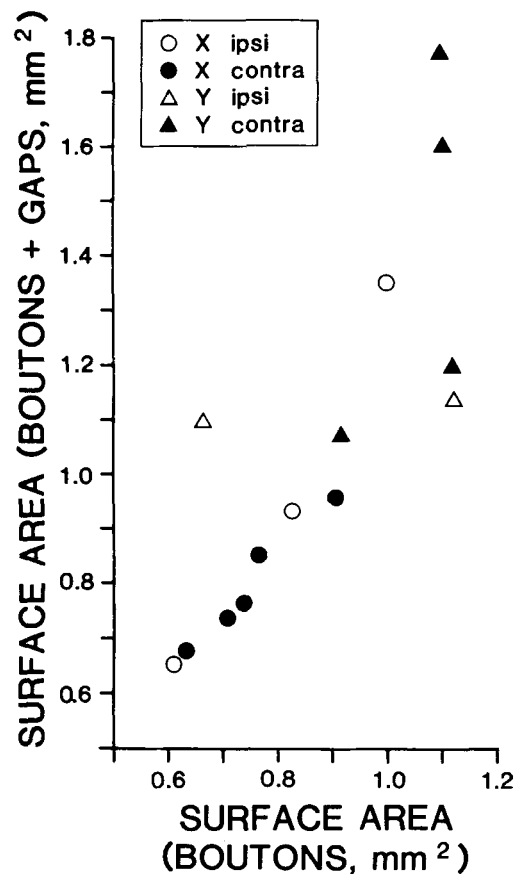


Fig. 17. Scatter plot of the surface areas of eight X- and six Y-cell arbors in layers IV and III. The abscissa plots the surface area covered by the boutons, not including any terminal free gaps, and the ordinate plots the total extent of the arbors (boutons plus terminal free gaps). Although there is some overlap along the ordinate, Y-cell arbors were significantly larger than are X-cell arbors. The number of points (14) is smaller than the number of reconstructed axons (19), because major distortions in the summary reconstructions of five arbors made it impossible to measure accurately their surface areas.

Fig. 16. Reconstruction of a Y-cell axon with a projection throughout layer IV. The cell's off-center receptive field,  $3.4^\circ$  in center diameter, was driven through the contralateral eye and was located  $32^\circ$  from the vertical meridian and  $10^\circ$  below the horizontal zero parallel. It responded nonlinearly to the grating, discharged vigorously to a fast moving disk, and had an (OX - OR) latency of 1.7 msec. This is the longest latency difference we have observed for a Y-cell. A. Lower power drawing of the terminal arbor and injection site (arrow). B,C. Drawings of the location of the cell body in the middle third of lamina A and the extent of the dendritic and axonal filling of the cell. The soma size was  $497 \mu\text{m}^2$ . D. Higher power reconstructions of the terminal arbor in four consecutive sections through the field. Note the input throughout both divisions of layer IV. Due to the extensive vertical distortion in the summary reconstruction of this axon's arbor (A), we have not constructed a surface view or measured its lateral dimensions.

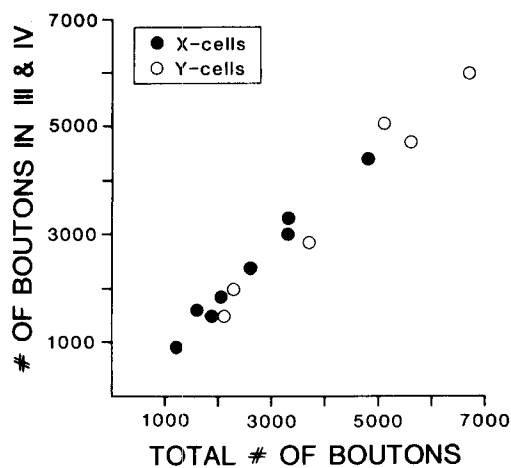


Fig. 18. Scatter plot of the numbers of boutons in eight X- and six Y-cell arbors. Despite substantial overlap, Y-cell axons distributed significantly more boutons than X-cell axons ( $P = .03$ ). The total number of boutons (abscissa) plotted against number of boutons in layers IV and III (ordinate) reveals that most of the boutons occupied layers IV and III. The number of points (14) is smaller than the number of reconstructed axons (19), because in 5 axons faint labeling of some distal processes made it difficult to visualize all of the boutons. The faintness was not restricted to one sublamina, however, and so does not affect the percentage values plotted in Figures 19B and 22A,B.

exceptions, the cells ranged from 200 to 415  $\mu\text{m}^2$  in area, with a median area of 295  $\mu\text{m}^2$  (open arrow). For comparison, the range and median value of soma sizes of the geniculate X-cells that were labeled intracellularly by Friedlander et al. ('81) are included in Figure 20A. A comparison of the two soma size distributions reveals that ours is lacking the smallest X-cells found by Friedlander et al. ('81). This difference in populations is significant ( $P < .001$ ), and it appears that we did not sample X-cells below 200  $\mu\text{m}^2$ . One explanation for this is that many of these small X-cells probably have axons whose diameters are too small for us to record or to impale, a problem that does not seem to affect recording and impaling of the parent somata (Friedlander et al., '81). This is consistent with the above observation that axon diameter is related to cell body size among X-cells. An additional possibility is that some of the smaller X-cells may be interneurons that do not project to cortex (Lin et al., '77; LeVay and Ferster, '79; Geisert, '80; Fitzpatrick et al., '84). Not all are interneurons, however, because Friedlander et al. ('81) determined that many of the smallest X-cells were relay neurons. The significance of these possible sampling biases will be considered in the Discussion.

All but two of our sample of 27 geniculate Y-cells that project to area 17 had their somata in lamina A or A1 of the LGN. The other two cells were located in lamina C and in the MIN but both were too poorly labeled to reconstruct their terminal arbors in cortex. The soma sizes of 40 retrogradely labeled Y-cells in the A-laminae are shown in Figure 20B. This includes Y-cells projecting to area 17, area 18, or to both areas, as well as Y-cells of unknown termination. The Y-cells had somata ranging from 205 to 675  $\mu\text{m}^2$ , with a median size of 410  $\mu\text{m}^2$  (open arrow in Fig. 20B). These values correspond well to the range and median values of the geniculate Y-cells injected by Friedlander et al. ('81), and no difference between populations was

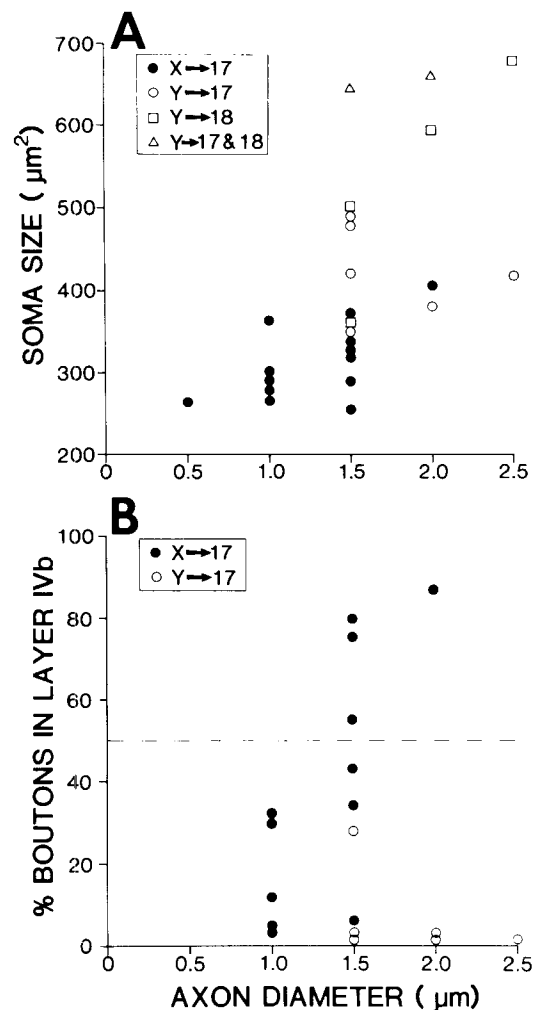


Fig. 19. Scatter plots of the relationships among axon diameter, soma size, and laminar projections. A. Axon diameter vs. soma size among 13 X- and six Y-cells that projected to area 17. For comparison, six Y-cells that projected to area 18 or to both areas are included. In general, there is a significant correlation ( $r = .58$ ,  $P < .01$ ) between axon diameter and soma size. This correlation also holds for X-cells, but not for the Y-cells (see text). In general, Y-cells have larger axons than do X-cells ( $P < .001$ ). Note the marked overlap between X- and Y-cell axons at 1.5 to 2.0  $\mu\text{m}$ . B. Axon diameter vs. sublamina of termination in layer IV of area 17. Among X-cells, no relationship exists between these two variables. All Y-cell axons, irrespective of diameter, project most heavily to layer IVa. The number of Y-cells that project to area 17 (six) shown in A and B is smaller than the number reconstructed (seven), because the parent axon of one Y-cell was labeled too lightly to measure it accurately.

evident ( $P > .1$ ). This correspondence indicates that we accurately sampled the Y-cell population available in the A-laminae. Further, our findings confirm those of Friedlander et al. ('81) that Y-cells are significantly larger than X-cells ( $P > .001$ ) despite considerable overlap.

Figure 20C,D shows the soma sizes of Y-cells whose axons were traced to area 17 or to area 18, respectively. Despite overlap, Y-cells that projected to area 17 had significantly smaller somata than did those projecting to area 18 ( $P < .01$ ). However, even these smaller Y-cells that projected to area 17 were significantly larger than the X-cells projecting to area 17 ( $P < .001$ ).

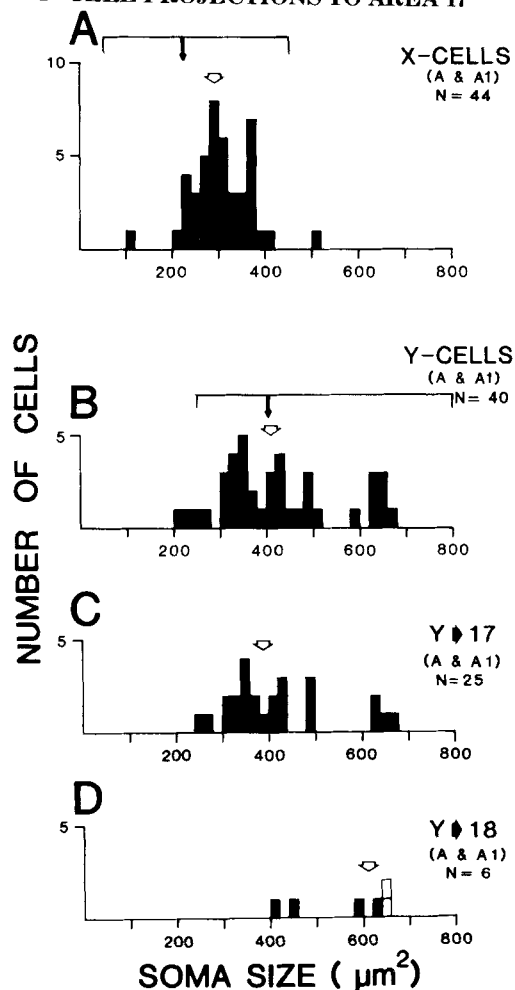


Fig. 20. Soma sizes (cross-sectional areas) of X- and Y-cells in the LGN that were retrogradely filled after injecting their axons in cortex. A. Soma sizes of 44 X-cells located in laminae A and A1. The total range of sizes is 112 to 508  $\mu\text{m}^2$ , with the majority ranging from 200 to 415  $\mu\text{m}^2$ , and the median size is 295  $\mu\text{m}^2$  (open arrow). The bracketed region above indicates the total range of X-cell soma sizes observed by Friedlander et al. ('81). These ranged from 75 to 440  $\mu\text{m}^2$ , with a median value of 230  $\mu\text{m}^2$  (filled arrow in A). Nearly all of the X-cells recovered in the present study had soma sizes within the upper half of the range observed by Friedlander et al. ('81). B. Soma sizes of 40 Y-cells located in laminae A and A1, which project to either area 17 or area 18. The range is 205 to 675  $\mu\text{m}^2$  and the median is 410  $\mu\text{m}^2$  (open arrow). The range (bracket) and median value (filled arrow) of the Y-cells injected by Friedlander et al. ('81) match well the distribution of our retrogradely filled Y-cells. C, D. Soma sizes of Y-cells that project to area 17 or to area 18. Median values are indicated by open arrows. The two open boxes in D indicate the soma sizes of two Y-cell axons that branched to innervate areas 17 and 18. Despite the large overlap, Y-cells that project to area 17 are significantly smaller than those projecting to area 18, or to both areas ( $P = .01$ ).

### Relationship between soma size and terminal arbors

It is generally assumed that a cell's soma size reflects the extent of its axon terminal field. This has been inferred largely from observations that monocular deprivation leads to smaller than normal somata in deprived laminae in the LGN and a marked reduction in the size of ocular dominance columns in layer IV of visual cortex (Wiesel and Hubel, '63; Guillery, '72; Shatz et al., '77; Hubel et al., '77; Shatz and Stryker, '78). However, no one has yet demon-

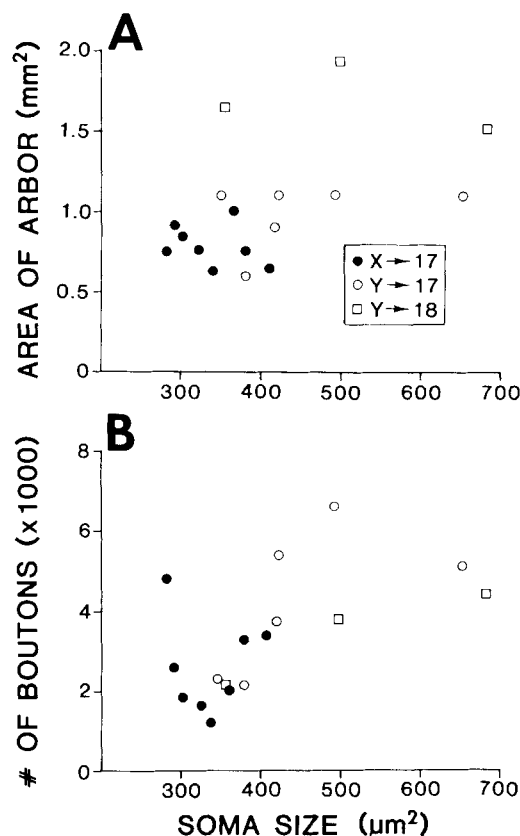


Fig. 21. Scatter plots of the relationships among soma size, terminal field area, and total number of boutons for eight X- and nine Y-cells that projected to area 17 or 18. A. Soma size vs. terminal field area. The ordinate plots the surface areas of the layer IV (and III) terminal arbors, not including any terminal-free gaps. See text for description. The number of cells shown is smaller than the total number of analyzed X- and Y-cells that projected to area 17 (12 and seven, respectively). For two X-cells, somata were not retrieved; for two others, the total extent of the terminal arbor was not visualized due to incomplete filling of the most distal processes. For one Y-cell axon (shown in Fig. 14), distortion in the final reconstruction of the terminal arbor precluded an accurate surface measure. The three Y-cell axons projecting to area 18 are presented in more detail in the following paper (Humphrey et al., '85). B. Soma size vs. total number of boutons. See text for description.

strated at the single cell level that soma size and axon extent are strongly related. We examined this relationship among eight X- and six Y-cells that projected to area 17 as well as three Y-cells that projected to area 18 (Fig. 21A). For all cells, there was a weak but significant correlation between soma size and axon terminal field area ( $r = .5$ ,  $P < .05$ ). However, within the subclasses of X- and Y-cell axons, no significant correlation was evident ( $r = .32$  for X-cells,  $r = .25$  for Y-cells, and  $P > .1$  for each). The correlation for the total cell sample might be an epiphenomenon of the tendency for Y-cells to have larger somata and axon arbors than do X-cells. It should be noted that variability among the Y-cells might be due to our not visualizing the full terminal arbors among those cells that project to both areas 17 and 18 (see the following paper for discussion of this possibility, Humphrey et al., '85). However, we are confident we have visualized the complete arbors of the X-cell axons in area 17, and we conclude that there is no clear

relationship between soma size and terminal arbor area among these cells. Preliminary analysis also indicates no relationship between soma size and terminal field volume.

We also investigated the relationship between soma size and total number of boutons in the axon terminal field (Fig. 21B). For X- and Y-cells as a whole, larger soma sizes reflect greater numbers of boutons ( $r = .56, P < .02$ ). However, again no significant relationship between these two variables exists within the X-cell group ( $r = -.02, P > .10$ ) or within the Y-cell group ( $r = .56, P > .05$ ). The same proviso as noted above for Y-cells, that variability might be due to different levels of incomplete filling of axon arbors, applies here as well. We nonetheless conclude that soma size is a poor predictor of the number of boutons within a cell's terminal arbor.

These findings do not rule out the possibility of correlated reductions in soma size and terminal field size or bouton numbers among single geniculate neurons following monocular deprivation. They do suggest, however, that if such correlations occur they may not represent cause and effect in any straightforward fashion.

### Relationship between soma location and laminar projection

As noted above, there was considerable heterogeneity in the sublaminar projections within area 17 of X-cells and, to some extent, of Y-cells. To our surprise, we found that the cells' laminar projections in cortex reflected the locations of their somata within the depth of the geniculate A-laminae. Figure 22A shows the soma locations of ten X-cells (filled circles) and seven Y-cells (open circles) within the depth of a schematic lamina A or A1. The lamina has been divided into dorsal, middle, and ventral thirds. The abscissa plots the percentage of boutons in the layer IV terminal arbor that were located in layer IVb. The figure reveals that X-cells that projected mainly to layer IVb had somata that were located in the central third of lamina A or A1. Conversely, those X-cells that projected most heavily above layer IVb tended to have somata lying in the dorsal or ventral thirds of lamina A or A1. A similar relationship holds for the Y-cells, although their laminar projections to layer IV differed from those of the X-cells. Y-cells that projected almost exclusively to layer IVa had somata in the dorsal or ventral third of lamina A or A1. The two Y-cell axons that also terminated substantially in layer IVb arose from somata in the middle third of lamina A or A1.

These positional relationships are illustrated differently in Figure 22B for the same cells. The abscissa is the same but the ordinate plots the percentage depth, or distance, of each cell from the center of its lamina (A or A1). The figure reiterates the observation that the depth at which an X-cell was located in lamina A or A1 was significantly correlated with the pattern of its terminal arbor in cortical layer IVa or IVb ( $r = -.63, P < .05$ ). The same is true for the Y-cells ( $r = -.76, P < .05$ ), although the specific relationship differs for X- and Y-cells. For instance, X-cell somata located in the middle third of lamina A or A1 possessed axons that terminated mainly in layer IVb; axons of similarly located Y-cell somata simply expanded their projections to include layer IVb while still maintaining their major projection to layer IVa. Thus, the sublaminar differences among the X- and Y-cell projections upon layer IV reflect an underlying sublaminar organization within the LGN.

The relationships revealed in Figure 22A,B do not seem to be due to any sampling biases in the locations of our

retrogradely labeled cells. Both groups of retrogradely labeled cells were roughly evenly distributed throughout all depths of the laminae (Fig. 22C,D). There was no tendency for Y-cells to be located more ventrally than X-cells in lamina A or A1 ( $P > .10$  on a  $\chi^2$  test), despite prior suggestions of this (Mitzdorf and Singer, '77; Bowling and Michael, '84). Also, there was no relationship between soma size and depth in the laminae. Since we seem to have accurately sampled the Y-cell population in these experiments (see Fig. 20B) this implies that Y-cells of all sizes are roughly evenly distributed throughout the depths of the A-laminae. Since we did not sample the smallest X-cells in the A-laminae (see Fig. 20A), we do not know how accurately Figure 22C reflects their depth distribution in the laminae. Likewise, we cannot predict from our data alone where these unsampled X-cells project in layer IV of striate cortex, if indeed they are all relay cells.

### Relationship between physiological properties and laminar projections

Other than the physiological differences between X- and Y-cells, we have observed no obvious physiological differences among the X- or Y-cells that were related to their different laminar projections in cortex. For example, despite their variable projections to area 17, all of the X-cell axons exhibited linear spatial summation to the counterphased gratings as well as other X-like response properties. It has been reported that cortical cells in layer IVa tend to have larger receptive fields and to respond to higher rates of stimulus movement than do cells in layer IVb (Bullier and Henry, '79c; Mustari et al., '82; Ferster and Lindstrom, '83). Examination of our physiological data, however, revealed no differences among X-cells terminating in upper and lower layer IV in terms of receptive field size or responsiveness to fast target movement. The above characteristics noted for layer IVa cortical cells may be due to the input from Y-cells, which have larger receptive fields and respond to higher stimulus velocities. We found no differences in the laminar terminations of on- and off-center geniculate cells, either X or Y, in area 17 (cf. Norton et al., '83, in tree shrew; and McConnell and LeVay, '83, in mink). Also, as Figure 22C,D shows, we observed no sublaminar pattern in the locations of on- and off-center cells within the depths of the geniculate A-laminae. This applies to our entire neuronal population and either subpopulation of X- or Y-cells ( $P > .10$  on a  $\chi^2$  test for each comparison).

It should be noted that these results do not rule out less obvious physiological correlates to soma position or axon projection among X-cells and Y-cells. The purpose of our physiological tests was to identify quickly X- and Y-cell axons using a battery of qualitative tests. Future quantitative analyses might reveal differences among geniculate cells in their spatial and temporal response properties that relate to their soma positions and laminar projections.

## DISCUSSION

Three major conclusions arise from this study. First, there is considerable overlap in the X- and Y-cell terminal arbors within layers IV and VI of area 17. Second, among both cell classes, soma location within the depth of geniculate lamina A or A1 is related to the sublaminar projection within layer IV. Third, most Y-cell terminal arbors have significantly larger surface areas and more boutons than do X-cell arbors. We will first reiterate the major sublaminar

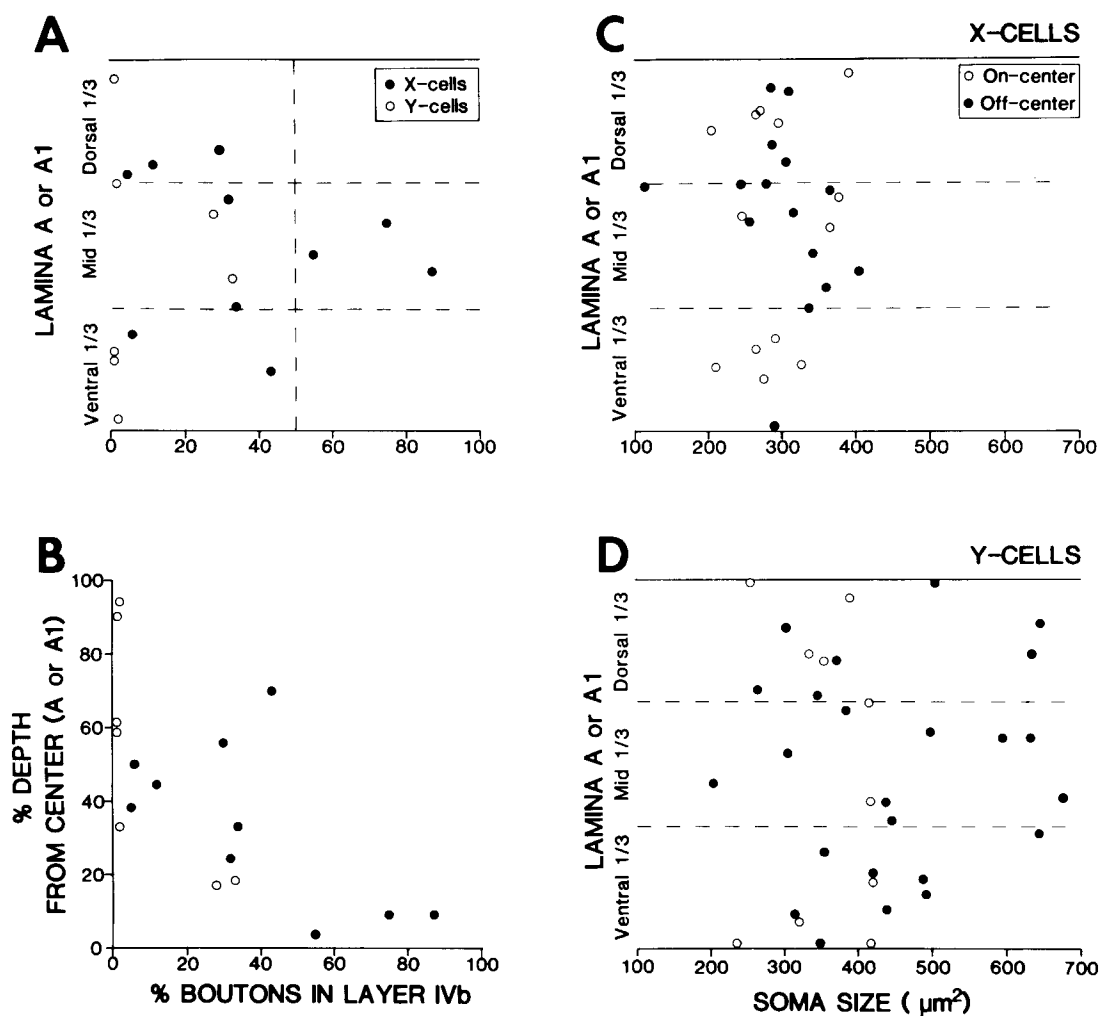


Fig. 22. Scatter plots showing the relationship for X- and Y-cells between cell body position in the LGN A-laminae and sublaminal projection within layer IV of area 17. A. Schematic diagram of a geniculate A-lamina (i.e., lamina A or A1). The dorsal and ventral borders of the lamina are indicated by the continuous, horizontal lines. Depth within the lamina is represented vertically and the lamina has been divided into thirds (horizontal dashed lines). The abscissa plots the percentage of boutons in the layer IV and layer III terminal field that occupy layer IVb. The vertical dashed line separates the population into cells with a denser projection to layer IVb (right) and cells with a denser projection above layer IVb (left), respectively. Those X-cells with a denser projection to layer IVb arise from the central third of the A-laminae. Those X-cells projecting more heavily to layer IVa and lower III are located within the dorsal and ventral thirds of the laminae. A similar relationship also holds for Y-cells. B. Different view of the same relationships as in A, with the same cells, symbols, and abscissa as in A. The ordinate plots the percentage distance of each cell from the center of the A-lamina. For example, cells located halfway between the center of a lamina and its dorsal or ventral borders have a standardized distance of 50%. The

plot reveals a significant correlation ( $r = -.67$ ;  $P < .01$ ) between soma position in the lamina and density of projection within layer IV. This relationship holds for the ten X-cells ( $r = -.63$ ;  $P < .05$ ) and for the seven Y-cells ( $r = -.76$ ;  $P < .05$ ). The number (ten) of X-cells in A and B is smaller than the number of reconstructed X-cell axons (12), because the somata of two axons were not recovered. C. Another schematic diagram of a geniculate A-lamina showing the depth locations of 28 retrogradely filled X-cells plotted against soma size. The somata were uniformly distributed throughout the depth of the A-laminae and showed no significant relationship between depth and soma size or center sign. Filled circles, off-center cells; open circles, on-center cells. D. Similar schematic diagram plotting soma depth vs. soma size for 34 Y-cells in the A-laminae. Y-cells were found throughout the depth of the A-laminae and no relationship was seen between soma depth, soma size, and center sign. The numbers of cells in C and D are smaller than those in Figure 20A and B, respectively, because the label in some somata completely faded before their depth in the LGN laminae could be measured.

patterns of the X- and Y-cell axons and then relate these to results from previous anatomical and physiological studies of the X- and Y-cell pathways. We will then discuss the implications of the relationships between soma position and terminal field location. The shapes and lateral extents of the terminal arbors will then be discussed in relation to the retinotopic mapping of cortex. Finally, the geniculate cell projection patterns seen here in the cat will be compared to those in the monkey.

### Projections of X- and Y-cells within layer IV of striate cortex

**Heterogeneity of X- and Y-cell afferent patterns.** X-cell axons exhibited a surprising heterogeneity in their layer IV projections. To date we have seen no X- or Y-cell axons whose terminal arbors were restricted exclusively to one or the other subdivisions of layer IV. This may not be surprising even among those largely restricted to one sublamina,

since the cytoarchitectonic boundary between upper and lower layer IV is itself not clear-cut (see Methods) and the dendrites of many layer IV cells freely cross this boundary (O'Leary, '41; Lund et al., '79; Gilbert and Wiesel, '79; Peters and Regidor, '81; Gilbert, '83; Martin and Whitteridge, '84).

While we have presented the X-cell axons as displaying three basic sublamina projection patterns in layer IV, we have no reason at present to believe that these reflect three separate classes of axon projection. Rather, there appears to be a continuum in sublamina projections, from those axons that are mainly restricted to one sublamina to those that arborize roughly equally throughout the depth of layer IV. This is supported by the results shown in Figure 22A,B, which reveal a large variation and no evidence of grouping in the sublamina distribution of X-cell boutons in layer IV. This is paralleled by a similar variability in the locations of X-cell somata within the depth of their A-laminae (Fig. 22A-C). We tentatively conclude that our sample of geniculostriate X-cells represents a single class with considerable variability.

Likewise, we cannot be certain whether the Y-cell sublamina projections reflect two separate classes (i.e., those innervating layer IVa vs. those terminating throughout layer IV) or form a continuum. Our sample of Y-cells in Figure 22A,B is smaller than that of the X-cells. However, as for the X-cells, we see no compelling evidence to support the conclusion of separate Y-cell subclasses. Perhaps a larger sample would alter this view.

While we see no subclasses of X- or Y-cell projections to layer IV, two recent series of studies suggest that subclasses may exist. In the first, Mastronarde ('83) reported that geniculate X-cells of the A-laminae can be divided into two groups, termed "normal" and "lagged" X-cells, on the basis of their connectivity with retinal X-cells and differences in the conduction times of their axons to cortex. "Normal" X-cells were antidromically activated by electrical stimulation of visual cortex with latencies of about 2.2 msec or less. For "lagged" X-cells, such latencies were  $\geq 1.9$  msec. The latencies of our axons to optic radiation stimulation are comparable to those of Mastronarde ('83), since both latency measurements revealed the geniculate cells' conduction times to cortex. All but two out of 113 optic radiation latencies of our X-cell axons were shorter than 1.8 msec, suggesting that virtually all of our X-cell axons arose from "normal" X-cells. We did not inject the two axons with longer latencies. Thus, the variability we have seen in our X-cell sample probably represents variability within the subclass of "normal" X-cells. Also, given the strong relationship between axon diameter and conduction velocity in vertebrate neurons (Hursh, '39; Rushton, '51; Waxman and Bennett, '72; Ritchie, '82), it seems likely that most of the slowly conducting axons of "lagged" X-cells were too fine in caliber for our electrodes to record and impale. This may also explain our failure to label the smallest population of X-cell somata that Friedlander et al. ('81) described (Fig. 20A). Since we have probably not sampled the "lagged" subclass of X-cells, it is possible that our data, which already indicate considerable variability among the geniculostriate X-cell projections, actually underestimate this variability. Another possibility is that the "lagged" subclass of X-cell innervates layer IVb and not layer IVa, so that we may have somewhat overestimated the extent of the X-cell input to layer IVa. Even so, this input to layer IVa is substantial.

The second set of experiments suggesting subclasses of X-cell afferents to area 17 is that of Einstein et al. ('83a,b). These authors reported that the axon terminals of LGN cells labeled by anterogradely transported, radiolabeled amino acids were of two morphological types. One contained round vesicles and formed asymmetric synaptic contacts with cortical cells throughout layer IV. The other contained pleomorphic vesicles and formed symmetric contacts with cortical cells, but these terminals were largely limited to layer IVb and the lower half of layer IVa. Einstein et al. ('83a,b) suggested that the former and latter types of terminals formed excitatory and inhibitory contacts, respectively, with cortical cells. Given their sublamina distribution in layer IV, the latter type presumably arose from a subpopulation of X-cells. We have shown that some X-cell axons terminated in layer IVb and lower layer IVa (Fig. 5D), but the ultrastructure of these and other injected axons remains to be determined. We also note that other authors (Colonnier and Rossignol, '69; Garey and Powell, '71; LeVay and Gilbert, '76; Winfield and Powell, '83; Tieman, '84) have reported that geniculocortical terminals are rather homogeneous morphologically, of the type with round vesicles forming asymmetric contacts.

**Relative number of synapses for X- and Y-cell afferents to layer IV.** Winfield and Powell ('83) have shown that single boutons in layer IVb, which these authors attributed to X-cell axons, tend to form a single synapse, while those in layer IVa, which were attributed to Y-cells, form about two synapses on average. While the number of synapses per bouton may differ between upper and lower layer IV it is not clear, given our results, that these reflect differences between X- and Y-cells. It is possible that both X- and Y-cell boutons in layer IVa make more synapses than those in IVb. Alternatively, Y-cell boutons may make more synapses than X-cell boutons irrespective of sublayer and some of the variability in synapses per bouton seen by Winfield and Powell ('83) in layer IVa might be due to the mixed X- and Y-cell input there. As a result, the difference between X- and Y-cell axons in numbers of synapses per bouton may be greater than estimated. This remains to be tested on physiologically identified axons. Further implications of our data and those of Winfield and Powell ('83) are considered below.

### Projections of X- and Y-cells within layer VI

Axons of X- and Y-cells varied considerably in the number of boutons distributed within layer VI and in their sublamina distribution there. To date we have been unable to relate this layer VI variability to variability in any other anatomical or physiological features. Some geniculate cells, by virtue of their greater input to layer VI, may much more strongly influence the activity of layer VI cells than do other geniculate cells. They thus may be in a position to exert a greater influence on the corticogeniculate system (Gilbert and Kelly, '75) or on the corticoclaustal system (Olson and Graybiel, '80; LeVay and Sherk, '81) than other LGN cells.

### Comparison with other studies

**Studies of axon projections.** Our finding that X- and Y-cells terminate throughout both divisions of layer IV is not in accord with earlier anatomical studies (Ferster and LeVay, '78; Bullier and Henry, '79c). As noted in the beginning of this paper, the conclusions from the anatomical study of Ferster and LeVay ('78) rest on the assumption

that Y-cells in the LGN are large, morphologically class 1 cells with relatively thick axons ( $\geq 2.0 \mu\text{m}$  in diameter) and that X-cells are smaller, morphologically class 2 cells with thinner axons ( $1.0$  to  $1.5 \mu\text{m}$  in diameter). These assumptions are not supported by more recent evidence (Friedlander et al., '81; the present study). Axon caliber is related to soma size, but some X-cells in the LGN have somata and axon diameters as large as do some Y-cells (Fig. 19A,B; Friedlander et al., '81). Axon caliber is thus not an unambiguous sign of functional class of geniculostriate axons, at least within the caliber range of  $1.5$  to  $2.0 \mu\text{m}$  where a large proportion of X- and Y-cell axons fall. Thus, part of the difference between our conclusion and that of Ferster and LeVay ('78) is due to their reliance on diameter to identify X- and Y-cell axons.

One additional discrepancy cannot so easily be explained. We found a number of X-cell axons with diameters of  $1.0$ – $1.5 \mu\text{m}$  that innervated layer IVa (Fig. 19B), but studies based on bulk-filling of geniculostriate axons (Ferster and LeVay, '78; Bullier and Henry, '79c) reported that no such fine-caliber axons innervated that sublayer. Given our ability to inject moderately small caliber ( $1.0 \mu\text{m}$ ) axons, differences between this and the previous studies do not appear to be attributable to our sampling dramatically different axonal populations. In general, it is difficult to interpret the results of extracellular injections of HRP made under cortex, particularly when a region of interest, such as layer IV, receives major, laminar specific inputs from non-geniculate sources, such as the claustrum (LeVay and Sherk, '83).

Gilbert and Wiesel ('79, '83), by use of the intracellular staining method, recently reported confirmation of a laminar segregation of X- and Y-cell axons in layer IV. Our different results concerning these cells' projections do not seem to be attributable either to differences in physiological classification criteria, since the property of linear or nonlinear summation was the criterion in both studies, or to assigning layer IV boundaries differently. However, Gilbert and Wiesel's ('79, '83) published sample of axons includes one X- and two Y-cells, and it might not be surprising, based on our data, to find one X-cell with boutons limited to layer IVb and two Y-cells with boutons limited to layer IVa. Nevertheless, we emphasize that our probability of sampling X-cell axons that project heavily to layer IVa is reasonably high, and therefore we do not believe that such axons represent a small minority or are easily missed with the intracellular staining method.

**Studies of cortical cells.** Bullier and Henry ('79a–c) used electrical activation of the retinogeniculostriate pathway to detect the type of afferent input onto extracellularly recorded cortical cells in area 17. They observed that many cells from lower layer III to the bottom of layer VI could be activated monosynaptically via the X- or Y-cell pathway. Our data are compatible with all of these observations and particularly help to explain the observation that some cells in upper layer IV and lower layer III could be monosynaptically activated by geniculocortical X-cells.

More recently, Martin and Whitteridge ('84) and Humphrey (unpublished results) replicated Bullier and Henry's ('79a–c) work using the intracellular staining method, which allowed a precise determination of the laminar location of each cortical cell and its dendrites. Monosynaptic geniculocortical activation via the X-cell pathway was observed for neurons located in lower layer III and throughout layers IV and VI. A number of these neurons in layers III and IVa

were pyramids whose basal dendrites did not extend in or near layer IVb. These cells must have been contacted fairly densely by X-cell axons similar to those that we have shown to project heavily into upper layer IV. Monosynaptic activation via the Y-cell pathway was observed in cells located in lower layer III, both divisions of layers IV and V, and lower layer VI, which is consistent with the pattern of Y-cell arbors we have observed. Finally, Ferster and Lindstrom ('83) used intracellular recording of postsynaptic potentials following electrical activation of the retino-geniculocortical pathway and also found monosynaptic activation to be prevalent among cells from mid-layer III to layer VIa. In all three of these studies a minority of layer V cells could be activated monosynaptically.

Regarding layer V, we have shown that a few X- and Y-cell axons distributed boutons throughout the layer (e.g., Figs. 9D, 11D, 13D), with the Y-cells contributing about three to four times as many boutons there as did the X-cells. For both classes, however, the numbers of boutons per axon were generally a small fraction of those found in the layer IV projection. It is difficult to imagine them strongly activating layer V cortical cells, unless a large number of these afferents converged onto a few layer V neurons. Alternatively, many of the monosynaptically driven layer V cells may have possessed basal or apical dendrites that encroached significantly into layers IV or VI (cf. Martin and Whitteridge, '84).

**Segregation of X- and Y-cell streams in cortex.** The X- and Y-cell streams are largely segregated through the LGN and, prior to our findings, were believed to terminate at different levels in layer IV. The overlap of X- and Y-afferents, particularly in layer IVa and lower layer III, raises the question of whether the two systems remain segregated or converge on single cells in cortex. Results of studies using electrical stimulation (Bullier and Henry, '79b,c; Ferster and Lindstrom, '83; Martin and Whitteridge, '84), chemical stimulation (Tanaka, '83b), or cross-correlation methods (Lee et al., '77; Tanaka, '83a) indicate surprisingly little convergence of the X- and Y-streams onto single cortical cells, either in layer IV or in other layers. Recently, Mullikin et al. ('84) also addressed this issue by searching for similarities in the spatiotemporal response properties of X- and Y-cells of the LGN and simple cells of the cortex. They, too, found little or no evidence of convergence of X- and Y-input onto single simple cells in lower layer III, layer IV, and layer VI. The lower half of layer IV contained almost exclusively X-like simple cells while the upper half of the layer contained both X-like and Y-like simple cells. Although other explanations are possible, this is certainly consistent with the pattern of terminations of X- and Y-cell arbors described here.

Finally, further evidence for a segregation of afferent streams in cortex comes from examination of the latencies of postsynaptic potentials recorded intracellularly following electrical stimulation of the retino-geniculocortical pathways. Ferster and Lindstrom ('83) observed that the response latencies associated with monosynaptic excitation and disynaptic inhibition in single cortical cells were highly correlated, suggesting that the excitatory and inhibitory postsynaptic potentials were mediated by afferents of similar conduction velocity and thus the same functional type. Although Ferster and Lindstrom ('83) themselves felt that they could not reliably distinguish between the X- and Y-cell streams in their study, their results suggest that these streams remain segregated beyond the first cortical cell.

Despite the substantial intermingling of X- and Y-cell arbors in layer IVa (and VI), the two groups selectively appear to contact different cortical cells. This should not seem surprising, since a similar phenomenon is evident in retinogeniculate circuitry. Despite intermingling of retinogeniculate X- and Y-cell axonal arbors in the A-laminae, nearly all geniculate cells there receive selective input from only one of these pathways (e.g., Cleland et al., '71; Hoffmann et al., '72). This indicates a great deal of specificity in the formation or maintenance of these synaptic circuits.

### Relationship between soma location and axon projection

**Soma depth in the A-laminae vs. axon arbor depth in layer IV.** One surprising result of this study was the relationship between geniculate cells' soma locations within lamina A or A1 and their sublaminar projections within layer IV of striate cortex. While both X- and Y-cells exhibited this relationship they expressed it in different ways, as shown in the summary diagram in Figure 23. X-cells in the central third of lamina A or A1 tended to project mainly to layer IVb while those in the dorsal and ventral thirds tended to project mainly to layer IVa and lower layer III or heavily throughout layer IV and lower layer III. On the other hand, Y-cells in the dorsal and ventral thirds of the laminae projected nearly exclusively to layer IVa and lower layer III. Y-cells in the central third still projected mainly to layer IVa and lower layer III, but also significantly invaded the full depth of layer IVb. Thus, the Y-cell projection emphasizes layer IVa. The portion of the X-cell projection that we have seen emphasizes both layers IVa and IVb. In contrast to the prior view that terminations within sublaminae of layer IV are determined by the functional class (X-cell or Y-cell) of axon, our data suggest that the location of the geniculate cell's soma may be as important as its functional class in determining its projection upon cortex.

An important proviso is that our X-cell sample may have been strongly biased in favor of axons arising from medium and large somata. We know neither where the smaller, unseen, X-cells were located in the A-laminae nor where they projected within layer IV. Results of current source density analysis (Mitzdorf and Singer, '78) suggest a substantial X-input to lower layer IV in cortex mediated by slowly conducting, presumably small caliber axons that might arise from these smaller X-cell somata. We would not necessarily expect these smaller X-cells to be restricted to one portion of lamina A or A1, since Hickey et al. ('77) have shown that small geniculate cells are distributed throughout the depth of the A-laminae. However, since some of the small cells may be interneurons whose depth distribution is unknown, these data do not rule out a non-uniform depth distribution of smaller relay X-cells in the A-laminae. Clearly, the number and location of these smaller relay X-cells and their projection patterns in cortex need to be determined.

**Functional significance of soma location.** It is not immediately obvious why a cell's laminar projection to cortex reflects its soma location in the LGN. Perhaps the more important structural feature in the LGN is the location of the cell's dendritic tree, which we have not adequately visualized. Most X- and Y-cell somata are located near the centers of their dendritic trees (see Figs. 19 and 20 of Friedlander et al., '81). Dendrite location in turn reflects the locations of the cells' inputs. For example, the retinal affer-

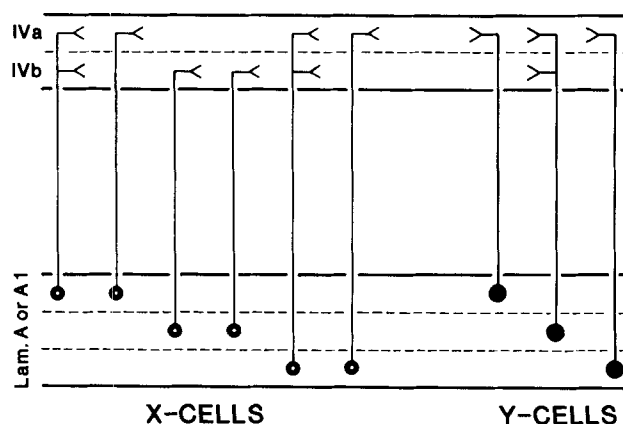


Fig. 23. Summary diagram of the relationship between soma location in the A-laminae and laminar projection in area 17. X-cells located in the dorsal and ventral thirds of the A-laminae tend to project either to layer IVa or throughout layer IV. X-cells located in the central third of the A-laminae project mainly to layer IVb. Y-cells located in the outer third of the A-laminae project mainly to layer IVa, while those in the central third project throughout layer IV. X- and Y-cells that project to layer IVa generally also arborize in the bottom 100 to 200  $\mu\text{m}$  of layer III (not illustrated).

ents terminate on a geniculate cell's dendrites, typically within 100  $\mu\text{m}$  of the soma (Hamos et al., '83; Wilson et al., '84). Differences in soma locations, then, may reflect differences in retinal afferent patterns.

Regarding the retinal afferents, Mitzdorf and Singer ('77), using current source density analysis, and Bowling and Michael ('84), using intracellular staining of retinogeniculate axons, reported a predominance of X-cell inputs to the dorsal halves of laminae A and A1, and Y-cell inputs to the lower halves. However, Sur and Sherman ('82, and unpublished findings) failed to replicate these anatomical results, and we found no significant differences in the locations of X- and Y-cell somata in the A-laminae (Fig. 22C,D). Bowling and Michael ('84) also reported differences in the shapes of the terminal fields of on- and off-center Y-cells from the retina. Off-center arbors were more conical, giving them a greater input to the bottoms of the A-laminae than to the tops. One might predict that this would result in more off-center Y-cells being located in the lower halves than in the upper halves of the A-laminae. Again, Sur and Sherman ('82, and unpublished findings) failed to observe this appearance of Y-cell arbors, and we found no such segregation among our retrogradely labeled Y- (or X-) cell somata (Fig. 22C,D).

At present there are no functional subdivisions within the A-laminae that explain the geniculocortical organization shown here. Soma location and axon projection might reflect other factors, such as subtle features of the cell's response properties, the pattern of extraretinal afferents, or the development of the geniculate laminae relative to the cortical layers.

### Relationship of arbors to retinotopic maps

Despite the fact that the X-cell terminal arbors are generally smaller in lateral extent than those of Y-cells, the extents of both the X- and Y-cell arbors seem quite large given the orderly retinotopic map across cortex and the relatively small receptive fields there. However, these ar-

bors are well within the range of the local scatter in the receptive fields of neighboring cortical cells. The distance required to move across striate cortex between two points at which the receptive fields do not overlap is about 2.5 mm in the cat (Albus, '75). Thus, there exist regions, defined as "spatial subunits" (Albus, '75), that are roughly 2.5 mm in diameter or nearly 5 mm<sup>2</sup> in surface area, and within which cortical cells have overlapping receptive fields. Individual X- and Y-cell terminal arbors in area 17 occupy only one-fifth and one-fourth, respectively, of a spatial subunit.

### Comparison with data from monkeys

The LGN of the macaque monkey consists of six laminae—four parvocellular and two magnocellular. How homologous these are to the cat LGN is not clear, but X-like and Y-like cells are present and appear to be partially segregated in the parvocellular and magnocellular laminae, respectively (Dreher et al., '76; Schiller and Malpeli, '78; but see Kaplan and Shapley, '82). On the basis of degeneration and autoradiographic studies (Hubel and Wiesel, '72; Henrickson et al., '78), the parvocellular laminae were found to project in area 17 to layers IV $\alpha$ , IV $\beta$ , and VI; the magnocellular laminae project to layers IV $\alpha$  and VI. Here, too, it is not clear what homologies exist between layer IV in the monkey and cat. Despite this, it is useful to compare our findings with those in the monkey.

Blasdel and Lund ('83) described the projections within macaque area 17 of single, HRP-filled axons believed to be from the LGN. Some were labeled by intra-axonal injection and others by extracellular injections in the white matter. The major differences between the cat and monkey axons are their sublaminal specificity and extent of lateral spread in layer IV. All axons that projected to layer IV $\beta$  in macaque terminated largely, though not exclusively, in either IV $\alpha$  or IV $\beta$ . Some of the latter arbors spilled over significantly onto the lower half of IV $\alpha$  (e.g., see Fig. 10 of Blasdel and Lund, '83), but for the most part, there was a far more complete sublaminal segregation in layer IV $\beta$  in monkey than we have found in the cat. In parallel with our evidence that laminar terminations in cat cortex relate to soma location in the lateral geniculate nucleus, the greater separation of afferents in the monkey may result from the more complete separation of their geniculate somata: in the cat, X- and Y-cells are intermingled in the A-laminae, while in the monkey, magno- and parvocellular cells reside in separate laminae. However, since many of the arbors described by Blasdel and Lund ('83) for the monkey were reconstructed from extracellular, bulk injections, particularly those in layer IV $\beta$ , some question remains as to whether all of the geniculocortical arbors in monkey layer IV $\beta$  are as well segregated. If geniculate X-cells in the cat are homologs of parvocellular cells in the monkey, these may be the best candidates in the monkey to show variability in projection patterns to cortex, and, as in the cat, bulk-filling may not adequately demonstrate this variability.

A clearer difference between cat and monkey is seen in the size of the geniculocortical arbors. The lateral extents of the layer IV arbors in the macaque are much smaller than are those in the cat. The larger, layer IV $\alpha$  arbors are roughly 0.5 mm<sup>2</sup> in area, or two to three times smaller than the Y-cell arbors in the cat; the smaller, layer IV $\beta$  arbors in monkeys are roughly 0.07 mm<sup>2</sup> in area, or about 11 times smaller than the X-cell arbors in cats. The IV $\alpha$  and IV $\beta$  arbors occupy roughly one-sixth and 1/45, respectively, of the spatial subunit (or "aggregate field," Hubel and

Wiesel, '77) in the monkey, which is roughly 3.1 mm<sup>2</sup> in area (Hubel and Wiesel, '74). Thus, using the spatial subunit as a scale, the "grain" of the geniculocortical projection is roughly an order of magnitude finer in the monkey than in the cat. This dramatic difference between the two species in the functional organization of the geniculostriate projection may be related to the vastly superior visual acuity of monkeys compared to cats (Hughes, '77; Uhlrich et al., '81).

### Diversity within the X- and Y-cell pathways

As we have noted repeatedly above, the X-cell arbors show much greater variability in their projection patterns upon layer IV than do the Y-cell arbors. Likewise, within the LGN, X-cells in the A-laminae have been divided into functionally different subgroups (Mastrorade, '83) and exhibit considerable structural diversity (Friedlander et al., '81). Y-cells in the A-laminae seem to be much more homogeneous both physiologically and morphologically (Friedlander et al., '81). Therefore, in the A-laminae and in area 17, the X-cell pathway exhibits more structural and functional heterogeneity than does the Y-cell pathway. The significance of this heterogeneity for information processing in striate cortex remains to be determined.

However, in the context of the lateral geniculate nucleus as a whole and its total cortical projections, the reverse seems true. The X-cell pathway basically involves just the A-laminae and area 17. The Y-cell pathway involves all major divisions of the lateral geniculate nucleus and many areas of extrastriate cortex in addition to area 17 (reviewed in Sherman and Spear, '82; Sherman, '84). The implications of this greater variability in the Y-cell pathway, in both cell location and axon projection, are not entirely clear. However, Y-cells in different regions of the lateral geniculate nucleus (e.g., lamina A and lamina C) exhibit differences in spatial and temporal resolution (Movshon, '81) and spatial and temporal contrast sensitivity functions (Frascella and Lehmkuhle, '83); they also appear to affect different classes of cells in visual cortex (Colby, '81). Thus the geniculocortical Y-cell pathway as a whole may also possess considerable functional and structural heterogeneity, but this heterogeneity takes a different form from that seen in the X-cell pathway. A challenge for future research is to understand the functional significance of this heterogeneity.

### ACKNOWLEDGMENTS

We thank Joan Sommermeyer, Angela Gero, and Pat Palam for outstanding technical assistance. This research was supported by Public Health Service grants EY04091, (A.L.H.), EY03038 (S.M.S.), and EY05688 (D.J.U.).

### LITERATURE CITED

- Adams, J.C. (1977) Technical considerations on the use of horseradish peroxidase as a neuronal marker. *Neuroscience* 2:141-145.
- Albus, K. (1975) A quantitative study of the projection area of the central and paracentral visual field in area 17 of the cat. *Exp. Brain Res.* 24:159-179.
- Bishop, P.O., W. Burke, and R. Davis (1962a) The interpretation of extracellular response of single lateral geniculate cells. *J. Physiol. (Lond.)* 162:451-472.
- Bishop, P.O., W. Kozak, and G.J. Vakkur (1962b) Some quantitative aspects of the cat's eye: Axis and plane of reference, visual field coordinates and optics. *J. Physiol. (Lond.)* 163:466-502.
- Bishop, P.O., G.H. Henry, and C.J. Smith (1971) Binocular interaction fields of single units in the cat striate cortex. *J. Physiol. (Lond.)* 216:39-68.

- Blasdel, G.G., and J.S. Lund (1983) Termination of afferent axons in macaque striate cortex. *J. Neurosci.* 3:1389-1413.
- Bowling, D.B., and C.R. Michael (1984) Terminal patterns of single, physiologically characterized optic tract fibers in the cat's lateral geniculate nucleus. *J. Neurosci.* 4:198-216.
- Boycott, B.B., and H. Wässle (1974) The morphological types of ganglion cells of the domestic cat's retina. *J. Physiol. (Lond.)* 240:397-419.
- Bullier, J., and G.H. Henry (1979a) Ordinal position of neurons in cat striate cortex. *J. Neurophysiol.* 42:1251-1263.
- Bullier, J., and G.H. Henry (1979b) Neural path taken by afferent streams in striate cortex of the cat. *J. Neurophysiol.* 42:1264-1270.
- Bullier, J., and G.H. Henry (1979c) Laminar distribution of first-order neurons and afferent terminals in cat striate cortex. *J. Neurophysiol.* 42:1271-1281.
- Cleland, B.G., M.W. Dubin, and W.R. Levick (1971) Sustained and transient neurones in the cat's retina and lateral geniculate nucleus. *J. Physiol. (Lond.)* 217:473-496.
- Cleland, B.G., W.R. Levick, and H. Wässle (1975) Physiological identification of a morphological class of cat retinal ganglion cells. *J. Physiol. (Lond.)* 248:151-171.
- Colby, C.L. (1981) Lateral geniculate nucleus origin of the corticotectal pathway in the cat. *Soc. Neurosci. Abstr.* 7:355.
- Colonnier, M., and R. Rossignol (1969) Heterogeneity of the cerebral cortex. In H.H. Jasper, A.A. Ward, and A. Pope (eds): *Basic Mechanisms of the Epilepsies*. Boston: Little, Brown, pp. 29-40.
- de Olmos, J.S. (1977) An improved HRP method for the study of central nervous connections. *Exp. Brain Res.* 29:541-551.
- Dreher, B., Y. Fukuda, and R.W. Rodieck (1976) Identification, classification and anatomical segregation of cells with X-like and Y-like properties in the lateral geniculate nucleus of old-world primates. *J. Physiol. (Lond.)* 258:433-452.
- Einstein, G., T.L. Davis, and P. Sterling (1983a) Ultrastructural evidence that two types of X-cell project to area 17. *Invest. Ophthalmol. Vis. Sci. [Suppl.]* 24:266.
- Einstein, G., T.L. Davis, and P. Sterling (1983b) Convergence on neurons in layer IV (cat area 17) of lateral geniculate terminals containing round or pleomorphic vesicles. *Soc. Neurosci. Abstr.* 9(2):820.
- Fernald, R.V., and R. Chase (1971) An improved method for plotting retinal landmarks and focusing the eyes. *Vision Res.* 11:95-96.
- Ferster, D., and S. LeVay (1978) The axonal arborizations of lateral geniculate neurons in the striate cortex of the cat. *J. Comp. Neurol.* 182:923-944.
- Ferster, D., and S. Lindstrom (1983) An intracellular analysis of geniculocortical connectivity in area 17 of the cat. *J. Physiol. (Lond.)* 342:181-215.
- Fitzpatrick, D., G.R. Penny, and D.E. Schmechel (1984) Glutamic acid decarboxylase-immunoreactive neurons and terminals in the lateral geniculate nucleus of the cat. *J. Neurosci.* 4:1809-1829.
- Fracella, J., and S. Lehmkuhle (1984) A comparison between Y-cells in the A-laminae and lamina C of the cat dorsal lateral geniculate nucleus. *J. Neurophysiol.* 52:911-920.
- Friedlander, M.J., C.-S. Lin, L.R. Stanford, and S.M. Sherman (1981) Morphology of functionally identified neurons in lateral geniculate nucleus of the cat. *J. Neurophysiol.* 46:80-129.
- Garey, L.J., and T.P.S. Powell (1971) An experimental study of the termination of the lateral geniculocortical pathway in the cat and monkey. *Proc. R. Soc. Lond. [Biol.]* 179:41-63.
- Geisert, E.E. (1980) Cortical projections of the lateral geniculate nucleus in the cat. *J. Comp. Neurol.* 190:793-812.
- Gilbert, C.D. (1983) Microcircuitry of the visual cortex. *Annu. Rev. Neurosci.* 6:217-247.
- Gilbert, C.D., and J.P. Kelly (1975) The projections of cells in different layers of the cat's visual cortex. *J. Comp. Neurol.* 163:81-106.
- Gilbert, C.D., and T.N. Wiesel (1979) Morphology and intracortical projections of functionally characterized neurones in the cat visual cortex. *Nature* 280:120-125.
- Gilbert, C.D., and T.N. Wiesel (1983) Clustered intrinsic connections in the cat visual cortex. *J. Neurosci.* 3:1116-1133.
- Guillery, R.W. (1966) A study of golgi preparations from the dorsal lateral geniculate nucleus of the adult cat. *J. Comp. Neurol.* 128:21-50.
- Guillery, R.W. (1972) Binocular competition in the control of geniculate cell growth. *J. Comp. Neurol.* 144:112-130.
- Hamos, J.E., D. Raczkowski, S.C. Van Horn, and S.M. Sherman (1983) The ultrastructural substrates for synaptic circuitry of an X retinogeniculate axon. *Soc. Neurosci. Abstr.* 9(2):814.
- Hendrickson, A.E., J.R. Wilson, and M.P. Ogren (1978) The neuroanatomical organization of pathways between the dorsal lateral geniculate nucleus and visual cortex in old world primates. *J. Comp. Neurol.* 182:123-136.
- Hickey, T.L., P.D. Spear, and K.E. Kratz (1977) Quantitative studies of cell size in the cat's lateral geniculate nucleus following visual deprivation. *J. Comp. Neurol.* 172:265-282.
- Hochstein, S., and R.M. Shapley (1976) Quantitative analysis of retinal ganglion cell classifications. *J. Physiol. (Lond.)* 262:237-264.
- Hoffmann, K.-P., J. Stone, and S.M. Sherman (1972) Relay of receptive field properties in dorsal lateral geniculate nucleus of the cat. *J. Neurophysiol.* 35:518-531.
- Hubel, D.H., and T.N. Wiesel (1972) Laminar and columnar distribution of geniculocortical fibers in the macaque monkey. *J. Comp. Neurol.* 146:421-450.
- Hubel, D.H., and T.N. Wiesel (1974) Uniformity of monkey striate cortex: A parallel relationship between field size, scatter, and magnification factor. *J. Comp. Neurol.* 158:295-306.
- Hubel, D.H., and T.N. Wiesel (1977) Ferrier Lecture: Functional architecture of macaque monkey visual cortex. *Proc. R. Soc. Lond. [Biol.]* 198:1-59.
- Hubel, D.H., T.N. Wiesel, and S. LeVay (1977) Plasticity of ocular dominance columns in monkey striate cortex. *Philos. Trans. R. Soc. [Biol.]* 278:377-409.
- Hughes, A. (1977) The topography of vision in mammals of contrasting life style: Comparative optics and retinal organization. In F. Crescitelli (ed): *Handbook of Sensory Physiology, Vol. VII/5: The Visual System of Vertebrates*. New York: Springer-Verlag, pp. 613-756.
- Humphrey, A.L., and D.J. Uhlrich (1984) The laminar projections of X- and Y-cell axons in layer IV of cat area 17 reflect the cells' locations within the depths of the A-laminae of the LGN. *Soc. Neurosci. Abstr.* 10(1):520.
- Humphrey, A.L., M. Sur, and S.M. Sherman (1982) Cortical axon terminal arborization and soma location of single, functionally identified lateral geniculate nucleus neurons. *Soc. Neurosci. Abstr.* 8(1):2.
- Humphrey, A.L., M. Sur, and S.M. Sherman (1983) Relationships between cell body size and axon terminal fields in single X- and Y-cells of the retina and lateral geniculate nucleus. *Soc. Neurosci. Abstr.* 9(2):813.
- Humphrey, A.L., M. Sur, D.J. Uhlrich, and S.M. Sherman (1985) Termination patterns of X- and Y-cell axons in the visual cortex of the cat: Projections to area 18, to the 17/18 border region, and to both areas 17 and 18. *J. Comp. Neurol.* 233:190-212.
- Hursh, J.B. (1939) Conduction velocity and diameter of nerve fibers. *Am. J. Physiol.* 127:131-139.
- Kaplan, E., and R.M. Shapley (1982) X and Y cells in the lateral geniculate nucleus of macaque monkeys. *J. Physiol. (Lond.)* 330:125-143.
- Krauth, J. (1983) The interpretation of significance tests for independent and dependent samples. *J. Neurosci. Methods* 9:269-281.
- Lee, B.B., B.G. Cleland, and O.D. Creutzfeldt (1977) The retinal input to cells in area 17 of the cat's cortex. *Exp. Brain Res.* 30:527-538.
- Lennie, P. (1980) Parallel visual pathways: A review. *Vision Res.* 20:561-594.
- LeVay, S. (1973) Synaptic patterns in the visual cortex of the cat and monkey: Electron microscopy of golgi preparations. *J. Comp. Neurol.* 150:53-86.
- LeVay, S., and D. Ferster (1979) Proportion of interneurons in the cat's lateral geniculate nucleus. *Brain Res.* 164:304-308.
- LeVay, S., and C.D. Gilbert (1976) Laminar patterns of geniculocortical projection in the cat. *Brain Res.* 113:1-19.
- LeVay, S., and H. Sherk (1981) The visual claustrum of the cat. I. Structure and connections. *J. Neurosci.* 1:956-980.
- Leventhal, A.G. (1979) Evidence that the different classes of relay cells of the cat's lateral geniculate nucleus terminate in different layers of the striate cortex. *Exp. Brain Res.* 37:349-372.
- Lin, C.-S., K.E. Kratz, and S.M. Sherman (1977) Percentage of relay cells in the cat's lateral geniculate nucleus. *Brain Res.* 131:167-173.
- Lund, J.S., G.H. Henry, C.L. MacQueen, and A.R. Harvey (1979) Anatomical organization of the primary visual cortex (area 17) of the cat. A comparison with area 17 of the macaque monkey. *J. Comp. Neurol.* 184:599-618.
- Martin, K.A.C., and D. Whitteridge (1984) Form, function, and intracortical projections of spiny neurones in the striate cortex of the cat. *J. Physiol. (Lond.)* 353:463-504.

- Mastrorade, D. (1983) Subtypes of X relay cells in the cat LGN can be distinguished solely by responses to visual stimuli. *Invest. Ophthalmol. Vis. Sci. [Suppl.]* 24:265.
- McConnell, S.K., and S. LeVay (1983) Geniculocortical afferents in the mink: Evidence for on/off and ocular dominance patches. *Soc. Neurosci. Abstr.* 9(2):617.
- Mitzdorf, U., and W. Singer (1977) Laminar segregation of afferents to lateral geniculate nucleus of the cat: An analysis of current source density. *J. Neurophysiol.* 40:1227-1244.
- Mitzdorf, U., and W. Singer (1978) Prominent excitatory pathways in the cat visual cortex (A 17 and A 18): A current source density analysis of electrically evoked potentials. *Exp. Brain Res.* 33:371-394.
- Movshon, J.A. (1981) Functional architecture in the cat's lateral geniculate nucleus. *Invest. Ophthalmol. Vis. Sci. [Suppl.]* 20:14.
- Mullikin, W.H., J.P. Jones, and L.A. Palmer (1984) Receptive field properties and laminar distribution of X-like and Y-like simple cells in cat area 17. *J. Neurophysiol.* 52:372-387.
- Mustari, M.J., J. Bullier, G.H. Henry (1982) Comparison of response properties of three types of monosynaptic S-cell in the cat striate cortex. *J. Neurophysiol.* 47:439-454.
- Norton, T.T., R. Kretz, and G. Rager (1983) On and off regions in layer IV of tree shrew striate cortex. *Invest. Ophthalmol. Vis. Sci. [Suppl.]* 24:265.
- O'Leary, J.L. (1941) Structure of the area striata of the cat. *J. Comp. Neurol.* 75:131-164.
- Olson, C.R., and A.M. Graybiel (1980) Sensory maps in the visual claustrum of the cat. *Nature* 288:479-481.
- Otsuka, R., and R. Hassler (1961) Uber Aufbau und Gliederung der corticalen Sehspahre bei der Katze. *Arch Psychiatr. Z. Ges. Neurol.* 203:212-234.
- Peichl, L., and H. Wässle (1981) Morphological identification of on- and off-centre brisk transient (Y) cells in the cat retina. *Proc. R. Soc. Lond. [Biol.]* 212:139-156.
- Peters, A., and J. Regidor (1981) A reassessment of the forms of non-pyramidal neurons in area 17 of the cat visual cortex. *J. Comp. Neurol.* 203:685-716.
- Ritchie, J.M. (1982) On the relation between fibre diameter and conduction velocity in myelinated nerve fibres. *Proc. R. Soc. Lond. [Biol.]* 217:29-35.
- Rosenquist, A.C., S.B. Edwards, and L.A. Palmer (1974) An autoradiographic study of the projections of the dorsal lateral geniculate nucleus and the posterior nucleus in the cat. *Brain Res.* 80:71-93.
- Rushton, W.A.H. (1951) A theory of the effects of fibre size in medullated nerve. *J. Physiol. (Lond.)* 115:101-122.
- Saito, H.-A. (1983) Morphology of physiologically identified X-, Y-, and W-type retinal ganglion cells of the cat. *J. Comp. Neurol.* 221:279-288.
- Sanderson, K.J. (1971) The projection of the visual field to the lateral geniculate and medial interlaminar nuclei in the cat. *J. Neurol.* 143:101-117.
- Schiller, P.H., and J.G. Malpeli (1978) Functional specificity of lateral geniculate nucleus laminae of the rhesus monkey. *J. Neurophysiol.* 41:788-796.
- Shatz, C.J., and M.P. Stryker (1978) Ocular dominance in layer IV of the cat's visual cortex and the effects of monocular deprivation. *J. Physiol. (Lond.)* 281:267-283.
- Shatz, C.J., S. Lindstrom, and T.N. Wiesel (1977) The distribution of afferents representing the right and left eyes in the cat's visual cortex. *Brain Res.* 131:102-116.
- Sherman, S.M. (1985) Functional organization of the W-, X-, and Y-cell pathways in the cat: A review and hypothesis. In J.M. Sprague and A.N. Epstein (eds): *Progress in Psychobiology and Physiological Psychology*, Vol. 11. New York: Academic Press (in press).
- Sherman, S.M., and P.D. Spear (1982) Organization of visual pathways in normal and visually deprived cats. *Physiol. Rev.* 62:738-855.
- Sherman, S.M., D.W. Watkins, and J.R. Wilson (1976) Further differences in receptive field properties of simple and complex cells in cat striate cortex. *Vision Res.* 16:919-927.
- So, Y.T., and R. Shapley (1979) Spatial properties of X and Y cells in the lateral geniculate nucleus of the cat and conduction velocities of their inputs. *Exp. Brain Res.* 36:533-550.
- Stanford, L.R., M.J. Friedlander, and S.M. Sherman (1983) Morphological and physiological properties of geniculate W-cells of the cat: A comparison with X- and Y-cells. *J. Neurophysiol.* 50:582-608.
- Stanford, L.R., and S.M. Sherman (1984) Structure/function relationships of retinal ganglion cells in the cat. *Brain Res.* 297:381-386.
- Stone, J., B. Dreher, and A. Leventhal (1979) Hierarchical and parallel mechanisms in the organization of visual cortex. *Brain Res. Rev.* 1:345-394.
- Sur, M., and S.M. Sherman (1982) Retinogeniculate terminations in cats: Morphological differences between X- and Y-cell axons. *Science* 218:389-391.
- Tanaka, K. (1983a) Cross-correlation analysis of geniculostriate neuronal relationships in cats. *J. Neurophysiol.* 49:1303-1318.
- Tanaka, K. (1983b) Distinct X- and Y-streams in the cat visual cortex revealed by bicuculline application. *Brain Res.* 265:143-147.
- Tieman, S.M. (1984) Effects of monocular deprivation on geniculocortical synapses in the cat. *J. Comp. Neurol.* 222:166-176.
- Uhrlich, D.J., E.A. Essock, and S. Lehmkuhle (1981) Cross-species correspondence of spatial contrast sensitivity functions. *Behav. Brain Res.* 2:291-299.
- Wässle, H., L. Peichl, and R.-B. Illing (1981a) Morphology and mosaic of on- and off-beta cells in the cat retina and some functional considerations. *Proc. R. Soc. Lond. [Biol.]* 212:177-195.
- Wässle, H., L. Peichl, and B.B. Boycott (1981b) Morphology and topography of on- and off-alpha cells in the cat retina. *Proc. R. Soc. Lond. [Biol.]* 212:157-175.
- Waxman, S.G., and M.V.L. Bennett (1972) Relative conduction velocity of small myelinated and non-myelinated fibres in the central nervous system. *Nature* 238:217-219.
- Wiesel, T.N., and D.H. Hubel (1963) Effects of visual deprivation on morphology and physiology of cells in the cat's lateral geniculate body. *J. Neurophysiol.* 26:978-993.
- Wilson, J.R., M.J. Friedlander, and S.M. Sherman (1984) Fine structural morphology of identified X- and Y-cells in the cat's lateral geniculate nucleus. *Proc. R. Soc. Lond. [Biol.]* 221:411-436.
- Winfield, D.A., and T.P.S. Powell (1983) Laminar cell counts and geniculocortical boutons in area 17 of cat and monkey. *Brain Res.* 277:223-229.